AAS 18-142

# RE-EVALUATING ORION'S RELATIVE NAVIGATION FILTER DESIGN FOR NASA'S FUTURE EXPLORATION MISSIONS

**David Woffinden[*], Renato Zanetti[†], Kirsten Tuggle[‡], Christopher D'Souza[§], Peter Spehar[¶]**

The vision of human exploration introduced by the Constellation Program over a decade ago demanded extensive capability from the Orion spacecraft. One of the critical flight elements included automated and piloted rendezvous and docking with multiple vehicles in Low Lunar Orbit (LLO) and Low Earth Orbit (LEO). To support the necessary rendezvous, proximity operations, and docking (RPOD) requirements, the design and development of the relative navigation system began. Following the cancellation of the Constellation Program and subsequent shifts in NASA's near term exploration goals, the need for the crewed Orion vehicle to perform RPOD was postponed along with the relative navigation filter development. Recently, NASA has begun procuring docking hardware to support upcoming exploration missions (EM) and the need to investigate Orion's rendezvous and docking capability has resurfaced. This paper revisits the relative navigation filter design and re-evaluates the selected formulation in context of past and current space programs, analyzes the performance and trades between different filter designs, and demonstrates the filter's performance in context of the proposed rendezvous and docking concept of operations (ConOps) envisioned for establishing a deep space gateway (DSG) in a lunar near rectilinear halo orbit (NRHO).

## INTRODUCTION

The ability to successfully perform rendezvous, proximity operations, and docking (RPOD) has been the cornerstone of human space exploration since its inception. At the heart of the execution of RPOD has been the ability to perform relative navigation with respect to the target vehicle. The first RPOD activities for the Orion program are expected to occur during NASA's Exploration Mission 3 (EM-3) with one of the target vehicles scheduled to launch in advance on EM-2. Planning and design for the Orion relative navigation filter has resumed since the last implementation in 2009 [1]. Given changes to both the Orion program and future mission objectives, this effort focuses on re-evaluating the Orion relative navigation filter design in context of lessons learned from past spaceflight programs while looking toward the future for Orion to achieve unprecedented levels of automation and mission flexibility. The challenge is to understand and apply best practices developed over the past several decades but strive to foresee unique challenges associated with missions flown decades into the future.

This work focuses on the formulation of the relative navigation translational filter. Determining both the number and type of states to most effectively support Orion RPOD activities becomes the central emphasis. The first section outlines the relative navigation filter design assumptions with regards to the rendezvous and docking concept of operations anticipated for the upcoming Orion exploration missions. The second section presents various filter formulation design options and discusses the advantages and disadvantages of each approach in context of past and current spaceflight programs along with their theoretical merit. The third section derives the framework to systematically compare the performance of each design option in a

[*]GN&C Autonomous Flight Systems Engineer, NASA JSC, Aeroscience and Flight Mechanics Division, david.c.woffinden@nasa.gov
[†]Asst Professor, Department of Aerospace Engineering and Engineering Mechanics, University of Texas at Austin, renato@utexas.edu
[‡]Ph.D. Student, Department of Aerospace Engineering and Engineering Mechanics, University of Texas at Austin, ktuggle@utexas.edu
[§]Navigation Technical Discipline Lead, NASA JSC, Aeroscience and Flight Mechanics Division, chris.dsouza-1@nasa.gov
[¶]Orion RPOD Lead, NASA JSC, Aeroscience and Flight Mechanics Division, peter.t.spehar@nasa.gov

qualitative manner. The fourth section evaluates and compares four different filter designs as applied to Orion's EM-3 rendezvous flight phases. The final section concludes with summarizing key trends and design recommendations moving forward.

## ORION RELATIVE NAVIGATION FILTER DESIGN ASSUMPTIONS

The relative navigation filter design encompasses several facets including the filter's 1) architecture, 2) formulation, 3) implementation, and 4) development environment. The filter architecture specifies the number of filters, the different types of filters, and their interaction with one another, sensor hardware, other GN&C subsystems, and flight software executive functions. The filter formulation determines the number and type of states and determines the fundamental filter equations to ensure adequate integrated system performance. The filter implementation selects the particular filtering techniques (Extended Kalman Filter, Square Root Filter, UDU factorization, Unscented Kalman Filter, etc. ) for executing the fundamental filtering functions and measurement processing to improve robustness, throughput constraints, and numerical stability. Lastly, the filter development environment addresses the coding language and processes adopted for flight software standards. The filter formulation design is the focus of this paper.

To begin identifying the proper filter formulation in context of upcoming Orion mission objectives, it becomes helpful to define the basic assumptions and the scope of application in terms of 1) target vehicle capabilities, 2) rendezvous domain and duration, 3) level of autonomy, and 4) rendezvous and docking operations. These in turn influence the type of measurements and sensors required along with the necessary guidance and targeting algorithms; both of which directly affect the filter formulation design. To provide a perspective that helps bound the anticipated needs and capabilities of Orion's relative navigation filter in the coming years and decades, first the emerging rendezvous and docking concepts of operations for EM-3 are introduced along with anticipated objectives for missions beyond EM-3. Based on the rendezvous and docking activities for EM3 and the speculated goals for subsequent missions, a summary is provided that outlines the basic assumptions to the key factors driving the relative navigation filter formulation design.

### Rendezvous and Docking Concept of Operations for EM-3

The second crewed Orion mission is schedule for the third exploration mission. The current concept for EM-3 entails the delivery of a habitation module to the Deep Space Gateway (DSG) [2] in an Earth-Moon Near Rectilinear Halo Orbit (NRHO) [3, 4]. Initially, DSG consists only of the power propulsion element (PPE) [5] launched previously with the EM-2 mission. Subsequent missions such as EM-4 and EM-5, would deliver other modules and elements. The vision for DSG is a crew-tended cislunar gateway that would be used as a staging point for both robotic and crewed lunar surface missions and for enabling travel to Mars. The NRHO trajectories maintained by DSG is a subset of the halo orbit families and is characterized by a close passage over one of the lunar poles. As depicted in Figure 1, the NRHO proposed for EM-3 is a southern NRHO which reaches the furthest distance from the Moon over the lunar south pole. The period of this particular NRHO is approximately seven days.

The rendezvous, proximity operations, docking, and undocking (RPODU) events are rather extensive for EM-3. There are two primary segments during the mission that require Orion to perform various rendezvous and proximity operations. Following the trans-lunar injection (TLI) burn highlighted in Figure 1(a), the first major RPODU sequence begins where Orion extracts the CPL (the habitation module) from the launch vehicle's Exploration Upper Stage (EUS) while enroute to the moon. Although the separation distance between Orion and the various targets are not significant, this segment poses several unique challenges.

Upon arrival at the moon, Orion executes the outbound power flyby (OPF) maneuver to strategically enter the NRHO near DSG with the NRHO insertion (NRI) maneuver shown in Figure 1(b). Once Orion has successfully entered the NRHO, it initiates a series of maneuvers to rendezvous and dock with DSG representing the second major RPODU activites. The nominal departure point for Orion to leave the NRHO is designated as the NRHO departure (NRD) maneuver which occurs approximately 10 days after NRI. When the time for the crew to return to Earth arrives, Orion undocks from DSG, separates itself, and performs the NRD burn. The NRD maneuver puts Orion on a trajectory to pass around the moon to execute the returned power flyby

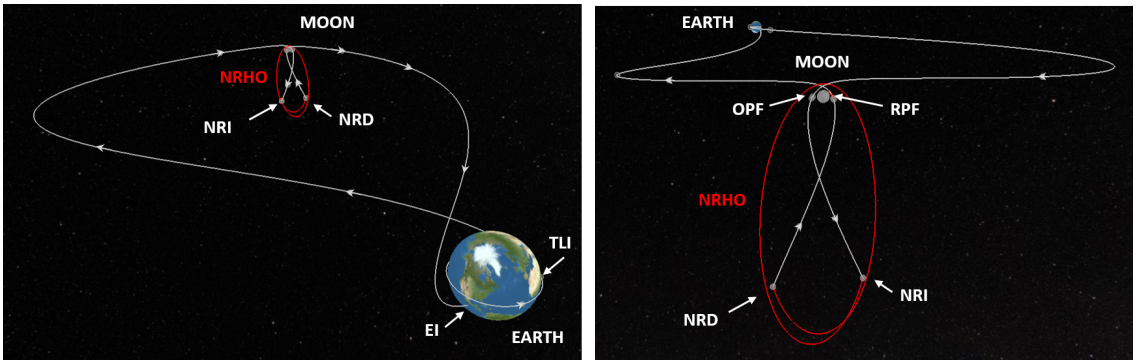


(a) Earth-to-Moon View

(b) Moon-to-Earth View

**Figure 1. The proposed Orion Exploration Mission-3 trajectory utilizing a southern Near Rectilinear Halo Orbit (NRHO).**

(RPF) maneuver which places Orion on a five day return trajectory to Earth. To begin understanding the performance required by the relative navigation filter to support these various RPODU activities, additional details are provided about the concept of operations for both extracting the CPL after TLI and docking with DSG in the NRHO.

**Orion Post-TLI Proximity Operations, Docking, and Undocking** The event sequence for Orion's proximity operations following TLI cutoff is summarized in Figure 2. After the TLI burn as depicted in Figure 2(a), Orion and EUS orient into a predetermined docking attitude shown in Figure 2(b) to accommodate thermal and power constraints. Once in the designated docking orientation, Orion separates from EUS, rotates 180 degrees, and station-keeps at a safe distance illustrated in Figure 2(c). Prior to station-keeping, it is assumed no relative measurements are available. Once Orion is at a safe holding distance, the EUS maneuvers to the Universal Stage Adapter (USA) separation attitude highlighted in Figure 2(d) and then releases the USA. Figure 2(e) emphasizes that the separation imparts a delta-v on the EUS which Orion responds to in order to maintain the desired relative station-keeping location on the designated docking axis.

Providing an accurate relative state estimate to the crew and automated system when EUS is in a non-docking orientation, while simultaneously estimating the relative motion with a *maneuvering* target that has separated into two elements, poses a variety of challenges that the relative navigation system must properly handle. As illustrated in Figure 2(k), the external surface of EUS contains reflective targets arranged in a pattern to optimize detectability given an assortment of relative EUS attitudes during the transposition sequence. A sample development pattern is provided in Figure 2(l). Besides having specially mounted refectors on EUS that can be tracked by the LIDAR to aid the relative state estimation problem, the current concept of operations also has the EUS attitude broadcasted to Orion via a communication link.

Once the USA is jettisoned, the CPL habitation module is now accessible. The EUS slews to the docking attitude represented in Figure 2(f). Orion's LIDAR acquires the docking reflectors and once the authority to proceed has been granted; Orion begins the approach and docking sequence to the CPL as shown in Figure 2(g). During the final approach, the relative attitude can be determined using the LIDAR tracking reflectors mounted near the docking port, by the crew visually monitoring the EUS using a centerline docking camera for lateral cues, or potentially an onboard vision navigation system processing the centerline docking camera images. When Orion has docked and secured the CPL, the EUS reorients the stack to point Orion/CPL in the necessary separation attitude in Figure 2(h). Upon separation depicted in Figure 2(i), the Orion/CPL stack rotates and departs while EUS performs the necessary disposal burns in Figure 2(j). The choreography between Orion, the target vehicles, the crew, and ground support includes a level of complexity that requires an adequate relative navigation solution to successfully meet mission objectives.

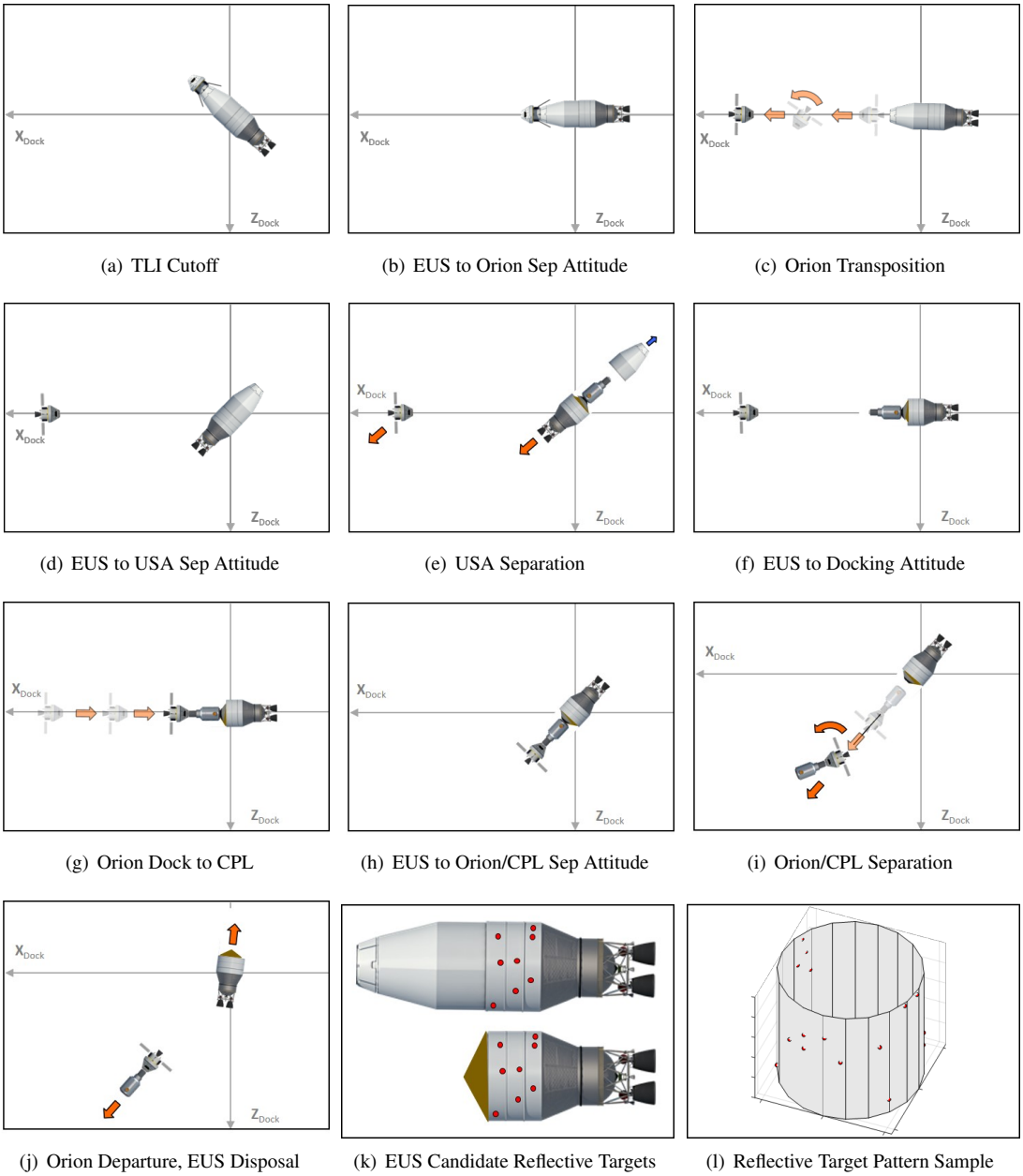


(a) TLI Cutoff (b) EUS to Orion Sep Attitude (c) Orion Transposition

(d) EUS to USA Sep Attitude (e) USA Separation (f) EUS to Docking Attitude

(g) Orion Dock to CPL (h) EUS to Orion/CPL Sep Attitude (i) Orion/CPL Separation

(j) Orion Departure, EUS Disposal (k) EUS Candidate Reflective Targets (l) Reflective Target Pattern Sample

**Figure 2. EM-3 Post-TLI Proximity Operations and Docking Event Sequence**

**Orion NRHO Rendezvous, Proximity Operations, and Docking** Several fundamental concepts specific to the NRHO rendezvous, proximity operations, and docking segment are illustrated in Figure 3. As depicted Figure 3(a), Orion enters the NRHO nearly along the docking axis of DSG at a distance up to several hundred kilometers and a relative velocity to ensure any resulting free drift or under-burn contingency scenarios do not pose a threat to DSG. A sequence of rendezvous maneuvers safely guides Orion to the predesignated docking axis in preparation for final approach. The current sensor configuration for Orion to support RPODU include long range S-band range and range-rate measurements from DSG; bearing angles from either the centerline docking camera, optical navigation camera, or star tracker; a LIDAR for close proximity operations; and a centerline docking camera for final approach and docking.

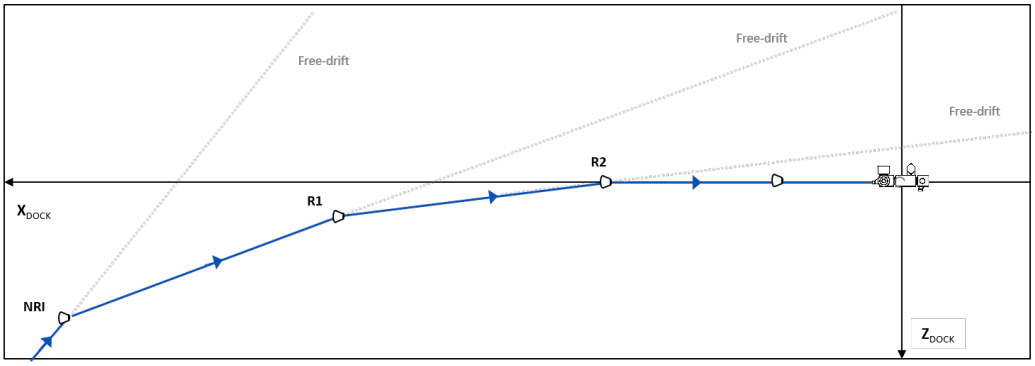


(a) Notional In-Plane NRHO Rendezvous, Proximity Operations, and Docking Trajectory

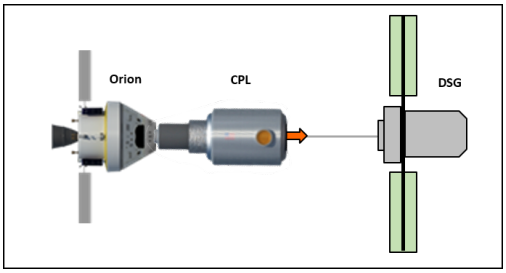


(b) EM3 Orion and CPL Docking Configuration

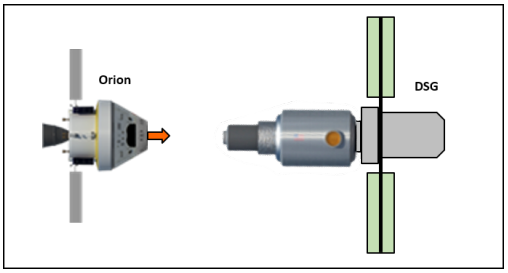


(c) Beyond EM3 Orion Notional Docking Configuration

**Figure 3. Notional EM-3 NRHO Proximity Operations and Docking Concepts**

As shown in Figure 3(b), the EM-3 Orion vehicle configuration has the CPL attached to the *front* of Orion covering the centerline docking camera and LIDAR. To ensure consistent measurements and performance, the CPL contains the same relative sensors mounted near its docking port. Not only does this attached configuration produce a challenge for sensing, it also limits the viewing conditions of the crew. For missions beyond EM-3 or for docking port relocation scenarios for EM-3, Figure 3(c) emphasizes the vehicle configuration without the CPL. For Orion, the relative navigation system design must account for these different configurations and support far-field rendezvous, near-field rendezvous, close proximity operations, docking, and undocking in a multi-body gravitational environment that enables the NRHO.

### Relative Navigation Assumption Summary

Identifying and selecting the proper filter formulation depends on several key factors such as 1) target vehicle capabilities, 2) rendezvous domain and duration, 3) level of autonomy, and 4) rendezvous and docking operations which in turn govern the available measurement types and the necessary guidance and targeting algorithms to support rendezvous and docking. A summary of the relative navigation assumptions is shown in Table 1. It highlights general examples of each category along with specific assumptions for EM-3 and anticipated capabilities for future Orion missions.

Given the basic RPOD assumptions in Table 1, the resulting available measurement types and potential guidance and targeting algorithms can be extrapolated which directly influence the relative navigation filter formulation. For example, the potential relative measurement types for EM-3 and beyond include relative range and range-rate, bearings to the target vehicle's centroid, angles to target features, LIDAR range and bearings, relative pose, visual odometry, and relative GPS. Candidate inertial measurements include GPS, bearings to celestial objects, celestial fixes, beacons, planetary features, and bearings to artificial satellites. These various measurement types must provide sufficient information to properly estimate both the relative and inertial states to support both relative and inertial guidance and targeting algorithms. For example, anticipated relative targeting and guidance algorithms for EM-3 include a modified glideslope [6] and inertial-

| | Examples | Orion Beyond EM-3 | Orion EM-3 |
|---|---|---|---|
| Target Vehicle | Cooperative or uncooperative, active or passive, attitude controlled or tumbling, known or unknown, maneuvering or drifting, communication assets or not | Cooperative or uncooperative, active or passive, attitude controlled or tumbling, known, maneuvering or drifting, communication assets or not | Cooperative, active, attitude controlled, known, maneuvering and drifting, communication assets |
| Domain | Low-Earth Orbit (LEO), Geostationary Orbit (GEO), Low-Lunar Orbit (LLO), Low-Mars Orbit (LMO), Distant Retro-grade Orbit (DRO), Near Rectilinear Halo Orbit (NRHO), Cis-lunar, Trans-Mars, Asteroid | Trans-lunar, Cis-lunar, Near Rectilinear Halo Orbit (NRHO), Low-Lunar Orbit (LLO), Low-Earth Orbit (LEO), Low-Mars Orbit (LMO), Trans-Mars | Trans-lunar and Near Rectilinear Halo Orbit (NRHO) |
| Autonomy | Automated, ground operated, ground support, ground over-site, local navigation assets, onboard crew monitoring, onboard crew navigating, onboard crew piloting | Automated, ground operated, ground support, ground over-site, local navigation assets, crew piloting, crew navigating, crew monitoring | Automated, ground support, and crew piloting |
| Operations | Far-field rendezvous, near-field rendezvous, close-proximity operations, docking, undocking, berthing, transposition, station-keeping, flyaround, docking port relocation | Far-field rendezvous, near-field rendezvous, close-proximity operations, docking, undocking, berthing, transposition, station-keeping, flyaround, docking port relocation | Far-field rendezvous, near-field rendezvous, close-proximity operations, docking, undocking, transposition, extraction, stationkeeping |

**Table 1. Orion RPODU Basic Assumptions and Application Summary**

relative targeting [7] with additional traditional relative algorithms such as CW-targeting, R-bar acquisition, TORVA, and other station-keeping algorithms envisioned for future exploration missions beyond EM-3. Inertial targeting algorithms for EM-3 include the two-level targeter and multi-body shooting methods. Upcoming missions may require other heritage inertial algorithms such as Lambert targeting, orbit phasing and altitude adjust burns, co-elliptic maneuvers, and plane change maneuvers,

## RELATIVE NAVIGATION TRANSLATIONAL FILTER FORMULATION OPTIONS

Given the potential suite of measurements along with the guidance and targeting algorithms anticipated for rendezvous, proximity operations, and docking; the objective is to determine the relative navigation filter formulation design that can most effectively utilize these measurements while supporting the desired mission operations. There are three general relative navigation filter formulations that are investigated and they include the: 1) relative, 2) dual inertial, and 3) inertial relative. This section defines each option and the potential variations within each approach. The advantages and weakness of each formulation are identified in context of their flight heritage on previous and current programs. Techniques that could be implemented to enhance and adopt each strategy are also provided.

### Relative-Only Filter

Since the goal is to estimate the relative state $\mathbf{x}_r$ between Orion or the chaser vehicle $\mathbf{x}_c$ and a target $\mathbf{x}_t$, the most straightforward option is, perhaps, a pure relative navigation filter. This solution is very intuitive and utilizes the minimum number of states required for relative navigation since no absolute states are included in the filter. It also results in optimal measurement updates to the relative state in the sense that its filter gain minimizes the expected squared error for the relative state estimate among the class of all linear estimators. This approach has been used for Space Shuttle's Rendezvous and Proximity Operations Program [6]

(RPOP) via Clohessy-Wiltshire (CW) equations [8] and ARGON [9] using relative orbital elements. Both versions require assumptions on the relative trajectory between the vehicles. A major disadvantage of the pure relative filter design is the requirement of such assumptions for propagation. For example, assuming only gravitational accelerations, the absolute states of the chaser and target evolve as

$$\dot{\mathbf{x}}_c = \mathbf{f}(\mathbf{x}_c) \qquad\qquad \dot{\mathbf{x}}_t = \mathbf{f}(\mathbf{x}_t) \tag{1}$$

such that the dynamics of the relative state, $\mathbf{x}_r = \mathbf{x}_t - \mathbf{x}_c$, can be defined as,

$$\dot{\mathbf{x}}_r = \dot{\mathbf{x}}_t - \dot{\mathbf{x}}_c = \mathbf{f}(\mathbf{x}_t) - \mathbf{f}(\mathbf{x}_c) = \mathbf{f}(\mathbf{x}_c + \mathbf{x}_r) - \mathbf{f}(\mathbf{x}_c) \tag{2}$$

To fully express the nonlinear dynamics of the relative state, knowledge of at least one of the absolute states such as the chaser state is needed, and a fully relative-only estimator without any absolute knowledge is not possible.

However, if approximations are allowed, a strict relative filter becomes implementable. First and foremost, assuming the chaser and the target are close, i.e. $\mathbf{x}_r$ is *small*, a first-order Taylor series centered at $\mathbf{x}_c$ can approximate the relative motion dynamics in Eqn 2.

$$\dot{\mathbf{x}}_r = \mathbf{f}(\mathbf{x}_c + \mathbf{x}_r) - \mathbf{f}(\mathbf{x}_c) \simeq \mathbf{f}(\mathbf{x}_c) + \mathbf{F}(\mathbf{x}_c)\,\mathbf{x}_r - \mathbf{f}(\mathbf{x}_c) = \mathbf{F}(\mathbf{x}_c)\,\mathbf{x}_r \tag{3}$$

There are several key points to note. First, the Jacobian of the dynamics, $\mathbf{F}(\mathbf{x}_c)$, is still evaluated at one of the absolute states (that of the chaser). Second, the usual EKF assumptions include the estimation error being small and linearized, not the estimated state. Using linearized dynamics is only valid in a small region around the chaser. This region is possibly larger using relative orbital elements rather than relative position and velocity

In order to reduce the dependency on $\mathbf{x}_c$, a further simplifications is possible when the target's orbit is nearly circular. By expressing the relative state in Local Vertical Local Horizontal (LVLH) coordinates, the Jacobian of the dynamics is not a function of all six degrees of freedom but rather a function of orbital radius only. This approach is so common that reference to a relative-only navigation system typically implies linearized CW dynamics.

Dependence of propagation of the relative state estimate on inertial information of one of the vehicles is an essential aspect of relative navigation. Although equations of motion for the relative state are known in form due to physical laws, they really represent a class of dynamical systems that varies over points in the state-space by which it is anchored (i.e. the inertial state of the chaser or target). This can even be seen in the linearized version above where evaluation of the Jacobian at one of the vehicle inertial states coincides with designation of the particular linear dynamics at each time among the class of all linear systems that can be generated by the Jacobian. This notion crucially implies that relative navigation is ultimately concerned with estimating variables ($\mathbf{x}_r$) that are only a portion of the states inherently representing the overall system ($\mathbf{x}_r$ and $\mathbf{x}_c$ or $\mathbf{x}_t$). Deficiencies of the pure relative filter are supported in that this design is an exercise in attempting to decouple an irreducibly coupled system. Absolute information for at least one of the vehicles is required for propagation of the relative state. Different architecture options are available based on the source of this absolute information.

### Dual-Inertial Filter

Another option is to estimate both the absolute state of the chaser and target in the onboard relative navigation solution, meaning $\mathbf{x} = \left[\mathbf{x}_c;\ \mathbf{x}_t\right]$. A dual-absolute filter is so commonly coordinated in the inertial frame that it is commonly referred to as a dual-inertial filter. It still optimally updates the relative state using relative measurements like the pure relative filter, but it now facilitates propagation using standard equations of motion. This option is clearly more computationally demanding, but, on the other hand, is also more accurate because no linearization of the dynamics occurs.

**Dual-Inertial Filter Observability** A drawback of this approach is that the full system (at least in its linearized form) is not strictly observable in the presence of relative measurements alone. Nonlinearities add observability, but the rate of convergence is usually low and possibly overwhelmed by process noise. Assume for simplicity that the relative state $\mathbf{x}_r$ is measured directly such that the measurement Jacobian equals, $\mathbf{H} = \begin{bmatrix}-\mathbf{I} & \mathbf{I}\end{bmatrix}$, and the measurement error variance is simply the identity matrix, $\mathbf{R} = \mathbf{I}$. In the absence of dynamics, the two states cannot be distinguished from each other since only their difference is measured.

For example, assume the initial state estimate has an estimation error covariance given by $\mathbf{P}_0$ shown below where there are no correlations between the chaser and target states. Processing the first ideal relative measurement, the correlation coefficient of the updated navigation error covariance $\mathbf{P}_1$ jumps from 0 to 1/2 in each component.

$$\mathbf{P}_0 = \begin{bmatrix}\mathbf{I} & \mathbf{0}\\ \mathbf{0} & \mathbf{I}\end{bmatrix} \rightarrow \mathbf{P}_1 = \begin{bmatrix}2/3\,\mathbf{I} & 1/3\,\mathbf{I}\\ 1/3\,\mathbf{I} & 2/3\,\mathbf{I}\end{bmatrix} \rightarrow \mathbf{P}_2 = \begin{bmatrix}3/5\,\mathbf{I} & 2/5\,\mathbf{I}\\ 2/5\,\mathbf{I} & 3/5\,\mathbf{I}\end{bmatrix} \rightarrow \ldots \rightarrow \mathbf{P}_n = \begin{bmatrix}1/2\,\mathbf{I} & 1/2\,\mathbf{I}\\ 1/2\,\mathbf{I} & 1/2\,\mathbf{I}\end{bmatrix}$$

If another measurement becomes available, the correlation coefficients of the covariance after the second update $\mathbf{P}_2$ becomes 2/3. After enough measurements $n$, the correlation coefficient of covariance $\mathbf{P}_n$ approaches one. From this point on, further measurements will not produce any improvement since the Kalman gain $\mathbf{K}_n$ becomes zero.

$$\mathbf{K}_n = \mathbf{P}_n\mathbf{H}^{\mathrm{T}}\left(\mathbf{H}\mathbf{P}_n\mathbf{H}^{\mathrm{T}} + \mathbf{R}\right)^{-1} = \begin{bmatrix}\mathbf{0}\\ \mathbf{0}\end{bmatrix}$$

The effects of the non-observable system are now clear. In the absence of process noise, the covariance of the relative state $\mathbf{P}_r$ becomes zero,

$$\mathbf{P}_r = \mathbf{H}\,\mathbf{P}_n\mathbf{H}^{\mathrm{T}} = \mathbf{0}$$

but an infinite number of measurements does not result in zero uncertainty of $\mathbf{P}_n$. Rather it results in the states being completely correlated.

Observations are modeled here to be independent and identically distributed (i.i.d.), meaning that measurements at all times are of the same probability distribution and are mutually independent. Because of this, the covariance after $n$ updates is given by

$$\mathbf{P}_n = \mathbf{P}_0 - \mathbf{P}_0\mathbf{H}^{\mathrm{T}}(\mathbf{H}\mathbf{P}_0\mathbf{H}^{\mathrm{T}} + \frac{1}{n}\mathbf{R})^{-1}\mathbf{H}\mathbf{P}_0 \tag{4}$$

$$\lim_{n\rightarrow+\infty}\mathbf{P}_n = \mathbf{P}_\infty = \mathbf{P}_0 - \mathbf{P}_0\mathbf{H}^{\mathrm{T}}(\mathbf{H}\mathbf{P}_0\mathbf{H}^{\mathrm{T}})^{-1}\mathbf{H}\mathbf{P}_0 \tag{5}$$

The results from Eqn. 5 simply state that in the absence of process noise all the measurement noise eventually averages out, and therefore the system is equivalent to processing a single perfect measurement. In general, $\mathbf{P}_\infty$ will be the result of one of three cases. First, if $\mathbf{H}$ is not of full row rank, a steady state solution does not exist. This makes sense because a non-full-rank $\mathbf{H}$ implies that the measurements are linear combinations of each other. A solution is not possible when measurements are perfect and combinations of each other. Second, when $\mathbf{H}$ is square and full rank (i.e. invertible), then $\lim_{n\rightarrow+\infty}\mathbf{P}_n = \mathbf{0}$. Finally when $H$ is of full row rank but not square $\lim_{n\rightarrow+\infty}\mathbf{H}\mathbf{P}_n\mathbf{H}^T = \mathbf{0}$ but this does not necessarily imply $\lim_{n\rightarrow+\infty}\mathbf{P}_n = \mathbf{0}$. In general, when the system is observable, the algebraic Riccati equation has at least one finite solution even in the presence of process noise (the system subject to process noise needs to be stabilizable for the solution to be unique).

A few comments about this results are in order. As mentioned above, dynamics and maneuvers can and do add some observability. In the presence of dynamics the measurement mapping matrix $\mathbf{H}$ is effectively replaced by $\mathbf{H}\mathbf{\Phi}$, where $\mathbf{\Phi}$ is the state transition matrix. Therefore dynamics effectively modifies $\mathbf{H}$ and can make the system observable. Notice that the linearized dynamics are also unobservable. Therefore, in the absence of maneuvers, observability is slow when nonlinearities are not pronounced, and process noise can overwhelm observability gained.The absolute uncertainty of the chaser and target are both reduced by processing relative-only measurements! Unfortunately this result does not necessarily hold with the inclusion

of process noise. Work exists analyzing estimation of inertial states using relative measurements [10,11]. The absolute uncertainty of the chaser and target are both reduced due to the fact that their initial correlation is zero. The covariance will eventually become singular or ill-conditioned [12].

**Dual-Inertial Filter Initialization** Initialization of the dual-inertial filter is an important consideration. Although the chaser state will be known from the absolute onboard filter, how is the initial estimate of the target obtained? Furthermore, what is the uncertainty in that estimate, and how is it correlated to the initial state of the chaser? If a completely independent estimate of the target state is available, then the initial covariance is block diagonal, and the analysis above holds. But that is not always the case. Sometime the absolute knowledge of the target is not available or is poorly known. Consider rendezvous with an asteroid as the target. The absolute state of the target is probably known with many kilometers of uncertainty while an initial relative state can be probably obtained much more accurately from the relative sensors.

Suppose a relative EKF is initialized using sensor measurements with the absolute state of the chaser uncorrelated with the sensed relative information. Hence the initial covariance will be

$$\mathbf{P}_0 = \begin{bmatrix} \mathbf{P}_c & \mathbf{P}_c \\ \mathbf{P}_c & \mathbf{P}_c + \mathbf{P}_r \end{bmatrix} \tag{6}$$

If a relative measurement is processed where $\mathbf{H} = \begin{bmatrix} -\mathbf{I} & \mathbf{I} \end{bmatrix}$, the updated covariance $\mathbf{P}_1$ equals,

$$\mathbf{P}_1 = \mathbf{P}_0 - \mathbf{P}_0\mathbf{H}^T(\mathbf{H}\mathbf{P}_0\mathbf{H}^T + \mathbf{R})^{-1}\mathbf{H}\mathbf{P}_0 \tag{7}$$

where it can be expressed as a function of the chaser state and the relative state uncertainty by substituting Eqn 6 for $\mathbf{P}_0$ and reducing.

$$\mathbf{P}_1 = \begin{bmatrix} \mathbf{P}_c & \mathbf{P}_c \\ \mathbf{P}_c & \mathbf{P}_c + \mathbf{P}_r \end{bmatrix} - \begin{bmatrix} \mathbf{0} & \mathbf{0} \\ \mathbf{0} & \mathbf{P}_r(\mathbf{P}_r + \mathbf{R})^{-1}\mathbf{P}_r \end{bmatrix} \tag{8}$$

The following conclusions are made. First, the chaser's absolute state and the correlations remain unchanged. In the presence of relative measurements alone, absolute information of the chaser is only obtained if independent absolute knowledge of the target is available at initialization. Even if such information is available, is it really needed to improve the absolute knowledge of Orion? Wouldn't the absolute filter still be running and be all that is needed? These questions compel definition of coordination between the absolute and relative filters. If they are to be isolated without feeding absolute states of Orion into the relative filter (which has been proposed for certification reasons and because much care needs to be taken in cascading filters), then again this is akin to decoupling the coupled system of relative motion. The relative filter would then carry its own, presumably different, absolute state of Orion (or the $T$), and improved knowledge of that state would serve to enhance propagation of the relative state. Whether that benefit is truly needed or not should be rigorously assessed and motivated in the current work. In a dual-inertial filter, the covariance can become ill-conditioned due *large* absolute errors that are almost the same and cancel out to produce *small* relative errors. To avoid this cancellation, if only the relative state is of ultimate concern, estimating one inertial and one relative state may prove better than two inertial states.

**Inertial-Relative Filter**

The absolute-relative or inertial-relative filter does precisely that and is theoretically equivalent to the dual-inertial formulation. The state is usually taken to be $\mathbf{x} = \begin{bmatrix} \mathbf{x}_t; & \mathbf{x}_r \end{bmatrix}$ for a couple of reasons. First, the target is usually non-thrusting, meaning it has simpler dynamics. Also, both the chaser and the relative state are affected by maneuvers and hence accelerometer errors, so it would be easier to avoid those correlations. However, if inertial relative measurements are available to the chaser vehicle during rendezvous (such as GPS, bearings to celestial objects, or celestial fixes) they are no longer directly related to the selected filter states; rather they will produce correlations between the relative and target state. Similar to the dilemma of having inertial states in the filter with only relative measurements, this would pose the challenge of having

relative states with inertial measurements. In this circumstance when inertial measurements to the chaser vehicle may be processed by the relative navigation filter, keeping the chaser inertial state along with the relative state may be preferred. Assume that the inertial-relative formulation uses the target state such that it is obtained from the dual-inertial state with a similarity transformation using the mapping matrix $\mathbf{M}$,

$$\mathbf{M} = \begin{bmatrix} \mathbf{I} & -\mathbf{I} \\ \mathbf{0} & \mathbf{I} \end{bmatrix} \tag{9}$$

Notice from the resulting measurement sensitivity matrix $\mathbf{H}$, the absolute state is not updated directly from the measurement but from its correlation to the relative state (which is an equivalent conclusion to what we drew in the dual-inertial case).

$$\mathbf{H} \leftarrow \mathbf{H}\mathbf{M}^{-1} = \begin{bmatrix} -\mathbf{I} & \mathbf{I} \end{bmatrix} \begin{bmatrix} \mathbf{I} & \mathbf{I} \\ \mathbf{0} & \mathbf{I} \end{bmatrix} = \begin{bmatrix} \mathbf{0} & \mathbf{I} \end{bmatrix} \tag{10}$$

The relative state here need not be directly propagated since the chaser absolute state can be formed from the target and relative states. Both vehicles can be directly propagated using standard equations of motion, and the relative state will be available as the difference between the two. This choice avoids modeling difficulties such as mechanizing relative drag. It should be noted that it also means that the absolute-relative and dual-inertial filters are not only mathematically equivalent but also operationally equivalent for the propagation phase. A question naturally arises in the case of initializing using relative measurements: if the absolute state is not directly measured and not directly needed, is it really needed to be carried in the filter?

**Relative Filter with External Absolute Parameter**

For filter formulation designs that deem carrying absolute variables in the relative filter unnecessary, options exist where the relative state is directly estimated and an absolute state can be either 1) considered (provided externally or propagated internally) or 2) provided externally to the relative filter (treated as errorless or as a simple white sequence with a tuning error covariance). A decision between these options depends on whether it is acceptable or not to ignore absolute error in Orion RPOD situations. Notice that an advantage here is maintaining a filter size that is the same as the pure relative filter. There do exist differences in computation between the two options in that the first requires additional operations and storage than the second to incorporate and store a covariance for the absolute state.

The Apollo and Shuttle relative filters [13, 14] made a simplification similar to that in the second option proposed with the absolute state estimates of one of the vehicles treated as available and errorless. However, the absolute state of the other vehicle rather than the relative state was estimated directly in the filter. Relative state estimates were again taken as the difference between the two vehicle estimates. The XSS-11 (eXperimental Satellite System-11) satellite [15] also utilized this type of filter. This design can be seen as a relaxation of the dual-inertial framework and is a suboptimal formulation. Though technically suboptimal, if one of the vehicle's inertial states are truly well known, then this design performs well at a lower computational burden (as evidenced through the history of Apollo and Shuttle missions). Such an assumption, however, is prohibitively limited for the wide purvey of RPOD scenarios imagined for Orion.

## RELATIVE NAVIGATION FILTER ANALYSIS APPROACH

Objectively evaluating the various filter formulation designs for multiple rendezvous profiles, in multiple rendezvous domains, with multiple targeting algorithms, utilizing multiple sensors in multiple configurations may initially appear overwhelming and impractical. Maybeck [16] addressed a similar challenge almost four decades ago. The solution he outlined using linear covariance analysis techniques has been adopted and become widely used for trajectory dispersion analysis [17–23] and evaluating navigation performance [24–26] for an assortment of aerospace applications [27–33] including onboard mission planning and navigation requirement generation [34–36]; but the original intent of comparing multiple filter designs and tuning filter parameters has been largely underutilized. This section outlines the techniques to analyze and compare the performance of an arbitrary number of filter formulation designs. This general approach is then applied to the specific filter formulations being investigated for Orion's relative navigation system.

**Performance Analysis Technique**

The basic concept of analyzing and comparing filter designs is highlighted in Figure 4 where $k$ different prospective Kalman filters process both discrete $\tilde{\mathbf{z}}$ and continuous $\tilde{\mathbf{y}}$ measurements generated in the *real world* environment. Each filter produces a navigation state estimate $\hat{\mathbf{x}}_k$ based on a particular model of the *real world* and can vary greatly due to model differences, variation in state dimension, and approximations. To make

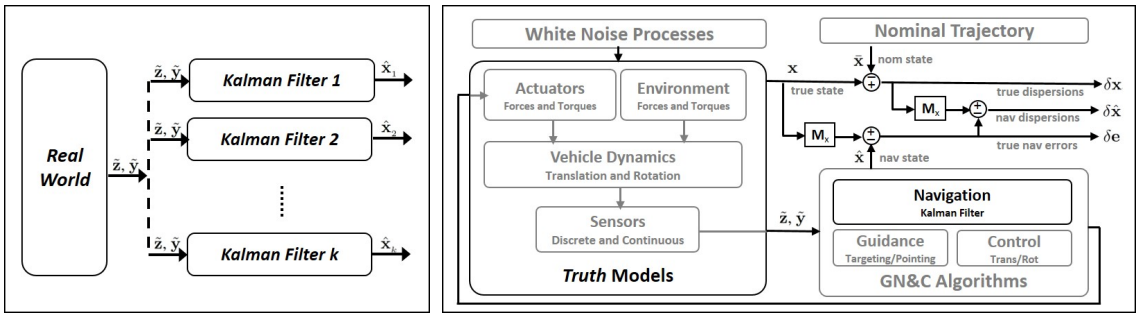


(a) Context of Filter Performance Analysis

(b) Performance Evaluation of a Kalman Filter Design

**Figure 4. Navigation Filter Design Performance Concepts**

design decisions, it is not requisite that each of these filters process measurements from actual sensors but rather the statistical representation of the estimation errors generated by each filter. By developing complete and high fidelity models of the system dynamics, these truth models can adequately test and evaluate each design as emphasized in Figure 4(b).

To directly compare the performance capability of each filter that has varying number and types of states, there are several performance metrics that may be utilized for evaluation which include the true trajectory dispersions $\delta\mathbf{x}$, the navigation dispersions $\delta\hat{\mathbf{x}}$, the true navigation error $\delta\mathbf{e}$, and the onboard navigation error $\delta\hat{\mathbf{e}}$. Traditionally, emphasis is made on the true navigation error of particular filter states $\delta\mathbf{e}$ such as position and velocity or derived performance states, $\delta\mathbf{e}_p = \mathbf{M}_p\delta\mathbf{e}$, such as range and range-rate. However, to capture how the navigation errors due to the filter design affect guidance, targeting, and control algorithms in following the prescribed trajectory profile, the true trajectory dispersions $\delta\mathbf{x}$ provide a valuable comparison criteria.

As depicted in Figure 4(b), the true dispersions $\delta\mathbf{x}$ are defined as the difference between the true state $\mathbf{x}$ and the nominal state $\bar{\mathbf{x}}$.

$$\delta\mathbf{x} \triangleq \mathbf{x} - \bar{\mathbf{x}} \tag{11}$$

$$\mathbf{D} = E\left[\delta\mathbf{x}\delta\mathbf{x}^{\mathrm{T}}\right] \tag{12}$$

The true state $\mathbf{x}$ is an $n$-dimensional vector that represents the *real world* environment or actual state. The nominal state $\bar{\mathbf{x}}$ is also an $n$-dimensional vector that represents the desired or reference state. The covariance of the environment dispersions, $\mathbf{D}$, indicates how precisely the system can follow a desired trajectory.

The navigation dispersions $\delta\hat{\mathbf{x}}$ are defined as the difference between the navigation state $\hat{\mathbf{x}}$ and the nominal state $\bar{\mathbf{x}}$. The navigation state is an $\hat{n}$-dimensional vector ($\hat{n} < n$) that represents the filter's estimated state.

$$\delta\hat{\mathbf{x}} \triangleq \hat{\mathbf{x}} - \mathbf{M}_x\bar{\mathbf{x}} \tag{13}$$

$$\hat{\mathbf{D}} = E\left[\delta\hat{\mathbf{x}}\delta\hat{\mathbf{x}}^{\mathrm{T}}\right] \tag{14}$$

The matrix $\mathbf{M}_x$ is an $(\hat{n} \times n)$ matrix that maps the estimated state in terms of the true and nominal state. The covariance of the navigation dispersions, $\hat{\mathbf{D}}$, reflect how precisely the onboard system thinks it can follow a prescribed reference trajectory.

The true navigation error $\delta\mathbf{e}$ is the difference between the environment and navigation states. It is also the difference between the environment and the navigation dispersions.

$$\begin{aligned} \delta\mathbf{e} &\triangleq \mathbf{M}_x\mathbf{x} - \hat{\mathbf{x}} = \mathbf{M}_x\delta\mathbf{x} - \delta\hat{\mathbf{x}} && (15) \\ \mathbf{P} &= E\left[\delta\mathbf{e}\delta\mathbf{e}^{\mathrm{T}}\right] && (16) \end{aligned}$$

The covariance of the true navigation error, $\mathbf{P}$, quantifies how precisely the onboard navigation system can estimate the actual state.

The onboard navigation error $\delta\hat{\mathbf{e}}$ itself is never computed, but it is used to develop the onboard navigation filter equations. It is defined as the difference between the design state, $\mathrm{x}$, and the navigation state $\hat{\mathbf{x}}$.

$$\begin{aligned} \delta\hat{\mathbf{e}} &\triangleq \mathrm{x} - \hat{\mathbf{x}} && (17) \\ \hat{\mathbf{P}} &= E\left[\delta\hat{\mathbf{e}}\delta\hat{\mathbf{e}}^{\mathrm{T}}\right] && (18) \end{aligned}$$

The covariance of the onboard navigation error, $\hat{\mathbf{P}}$, quantifies how precisely the onboard navigation system thinks it can determine the actual state. The performance of the onboard navigation system is determined by comparing $\hat{\mathbf{P}}$ to the actual navigation performance $\mathbf{P}$.

One approach of generating this statistical information is a Monte Carlo analysis where hundreds or thousands of samples, $N$, are generated by simulation and then the sample statistics are computed directly

$$\begin{aligned} \mathbf{D} &= \frac{1}{N-1}\sum \delta\mathbf{x}\delta\mathbf{x}^{\mathrm{T}} \\ \hat{\mathbf{D}} &= \frac{1}{N-1}\sum \delta\hat{\mathbf{x}}\delta\hat{\mathbf{x}}^{\mathrm{T}} \\ \mathbf{P} &= \frac{1}{N-1}\sum \delta\mathbf{e}\delta\mathbf{e}^{\mathrm{T}} \end{aligned}$$

The onboard navigation error covariance $\hat{\mathbf{P}}$ is obtained from the navigation filter covariance for each run. Unfortunately, this is a costly and time-consuming process. A more efficient technique to obtain the same statistical information but with a single run is using linear covariance analysis techniques [16, 17] by initializing, propagating, updating, and correcting an augmented state covariance matrix $\mathbf{C}$ and the onboard navigation covariance matrix $\hat{\mathbf{P}}$,

$$\mathbf{C} = E\left[\delta\mathbf{X}\delta\mathbf{X}^{\mathrm{T}}\right] \quad (19)$$

where the augmented state $\delta\mathbf{X}^{\mathrm{T}} = [\delta\mathbf{x}^{\mathrm{T}}\ \delta\hat{\mathbf{x}}^{\mathrm{T}}]$ consists of the true dispersions and the navigation dispersions. By pre- and post-multiplying the augmented state covariance matrix with the following matrices, the covariance matrices for the trajectory dispersions, navigation dispersions, and the navigation error can be obtained.

$$\begin{aligned} \mathbf{D} &= [\,\mathbf{I}_{n\times n},\ \mathbf{0}_{n\times\hat{n}}\,]\,\mathbf{C}\,[\,\mathbf{I}_{n\times n},\ \mathbf{0}_{n\times\hat{n}}\,]^{\mathrm{T}} \\ \hat{\mathbf{D}} &= [\,\mathbf{0}_{\hat{n}\times n},\ \mathbf{I}_{\hat{n}\times\hat{n}}\,]\,\mathbf{C}\,[\,\mathbf{0}_{\hat{n}\times n},\ \mathbf{I}_{\hat{n}\times\hat{n}}\,]^{\mathrm{T}} \\ \mathbf{P} &= [\,\mathbf{I}_{\hat{n}\times n},\ -\mathbf{I}_{\hat{n}\times\hat{n}}\,]\,\mathbf{C}\,[\,\mathbf{I}_{\hat{n}\times n},\ -\mathbf{I}_{\hat{n}\times\hat{n}}\,]^{\mathrm{T}} \end{aligned}$$

**Relative Navigation Filter Modeling** One approach for modeling an assortment of filter designs of various state dimensions is to first develop a filter implementation with the navigation state $\hat{\mathbf{x}}$ that includes the largest number of possible states relevant to the problem with the highest fidelity models such that the navigation state largely mimics the true states $\mathbf{x}$ in complexity and fidelity ($\hat{n} \leq n$). Although it would not be practical to implement, the results of this filter would represent the best possible performance. All other filter designs with the selected navigation states $\hat{\mathbf{x}}_k$ of $\hat{n}_k$-dimension ($\hat{n}_k \leq \hat{n}$) could be expressed as a function of the ideal navigation states $\hat{\mathbf{x}}$,

$$\hat{\mathbf{x}}_k = \hat{\mathbf{m}}_k(\hat{\mathbf{x}}) \quad (20)$$

As a result, the navigation dispersions $\delta\hat{\mathbf{x}}_k$ and onboard navigation error $\delta\hat{\mathbf{e}}_k$ of the proposed filter design can be expressed as a linear combination of the original navigation dispersions $\delta\hat{\mathbf{x}}$ and onboard navigation error $\delta\hat{\mathbf{e}}$,

$$\delta\hat{\mathbf{x}}_k = \hat{\mathbf{M}}_k \delta\hat{\mathbf{x}}, \qquad \delta\hat{\mathbf{e}}_k = \hat{\mathbf{M}}_k \delta\hat{\mathbf{e}} \tag{21}$$

where $\hat{\mathbf{M}}_k = \frac{\partial \hat{\mathbf{m}}_k}{\hat{\mathbf{x}}}|_{\bar{\mathbf{x}}}$. In this manner, the augmented state covariance matrix and the onboard navigation covariance matrix can be quickly modified to reflect each potential filter formulation,

$$\mathbf{C}_k = E\left[\delta\mathbf{X}_k \delta\mathbf{X}_k^{\mathrm{T}}\right], \qquad \hat{\mathbf{P}}_k = E\left[\delta\hat{\mathbf{e}}_k \delta\hat{\mathbf{e}}_k^{\mathrm{T}}\right] \tag{22}$$

where the augmented state corresponding to the $k$ filter formulation $\delta\mathbf{X}_k^{\mathrm{T}} = [\delta\mathbf{x}^{\mathrm{T}}\ \delta\hat{\mathbf{x}}_k^{\mathrm{T}}]$ consists of the true dispersions and the modified navigation dispersions. Substituting Eqn 21 into Eqn 22 produces the mapping between the original and modified covariance matrices,

$$\mathbf{C}_k = \mathbf{M}_k \mathbf{C} \mathbf{M}_k^{\mathrm{T}}, \qquad \hat{\mathbf{P}}_k = \hat{\mathbf{M}}_k \hat{\mathbf{P}} \hat{\mathbf{M}}_k^{\mathrm{T}} \tag{23}$$

where the augmented state covariance matrix mapping matrix $\mathbf{M}_k$ becomes

$$\mathbf{M}_k = \begin{bmatrix} \mathbf{I}_{n\times n} & \mathbf{0}_{n\times\hat{n}_k} \\ \mathbf{0}_{\hat{n}_k\times n} & \hat{\mathbf{M}}_k \end{bmatrix} \tag{24}$$

By appropriately applying these transformations for the initialization, propagation, update, and correction operations; it provides a mechanism to quickly and accurately evaluate the performance of $k$ filter formulation designs by merely defining the matrix $\hat{\mathbf{M}}_k$. For example, if the performance of the ideal filter is selected, then the mapping matrix is simply the identity, $\hat{\mathbf{M}}_k = \mathbf{I}_{\hat{n}\times\hat{n}}$. To establish the filter formulation mapping matrix $\hat{\mathbf{M}}_k$ for each reduced-state filter design, it is essential to first define the truth states $\mathbf{x}$ that provide the best *real world* model and the corresponding ideal filter states $\hat{\mathbf{x}}$.

**Rendezvous Truth and Navigation States** For rendezvous and docking the $n$-dimensional truth state vector consists of Orion's or the chaser vehicle states $\mathbf{x}_c$, the target vehicle states $\mathbf{x}_t$, and parameter states $\mathbf{x}_p$

$$\mathbf{x} = \left[\mathbf{x}_c;\ \mathbf{x}_t;\ \mathbf{x}_p\right] \tag{25}$$

The chaser states consist of the chaser's inertial position, velocity, attitude, and angular velocity. The target states also include the target's inertial position, velocity, attitude, and angular velocity. Depending on the sensors selected and analyzed, the parameter states will vary. They may include continuous measurement states $\mathbf{p}_{\tilde{\mathbf{z}}}$ such as gyro and accelerometer biases, scale factors, misalignments, and non-orthogonality terms; discrete measurement states $\mathbf{p}_{\tilde{\mathbf{z}}}$ such as LIDAR bearing and range biases and misalignments; impulsive translational burn states $\mathbf{p}_{\Delta\mathbf{v}}$; rotational control maneuver states $\mathbf{p}_{\boldsymbol{\tau}}$; and other pertinent states $\mathbf{p}_a$ necessary to properly model affects due to solar radiation pressure, planetary ephemeris, atmospheric drag, etc.

$$\mathbf{x}_c = \left[\mathbf{r}_c;\ \mathbf{v}_c;\ \mathbf{q}_i^c;\ \boldsymbol{\omega}_c^c\right] \tag{26}$$

$$\mathbf{x}_t = \left[\mathbf{r}_t;\ \mathbf{v}_t;\ \mathbf{q}_i^t;\ \boldsymbol{\omega}_t^t\right] \tag{27}$$

$$\mathbf{x}_p = \left[\mathbf{p}_{\tilde{\mathbf{z}}};\ \mathbf{p}_{\tilde{\mathbf{y}}};\ \mathbf{p}_{\Delta\mathbf{v}};\ \mathbf{p}_{\boldsymbol{\tau}};\ \mathbf{p}_a\right] \tag{28}$$

The resulting number of truth model states $n$ can be on the order of hundreds of states. The ideal navigation state $\hat{\mathbf{x}}$ is an $\hat{n}$-dimension state vector. For this development the number of navigation states $\hat{n}$ equals the number of truth states $n$ except for conditions when gyros are utilized.

$$\hat{\mathbf{x}} = \left[\hat{\mathbf{x}}_c;\ \hat{\mathbf{x}}_t;\ \hat{\mathbf{x}}_p\right] \tag{29}$$

In this circumstance, the chaser angular rate state is not included and the attitude model operates in model replacement mode.

$$\hat{\mathbf{x}}_c = \left[\hat{\mathbf{r}}_c;\ \hat{\mathbf{v}}_c;\ \hat{\mathbf{q}}_i^c\right] \tag{30}$$

$$\hat{\mathbf{x}}_t = \left[\hat{\mathbf{r}}_t;\ \hat{\mathbf{v}}_t;\ \hat{\mathbf{q}}_i^t;\ \hat{\boldsymbol{\omega}}_t^t\right] \tag{31}$$

$$\hat{\mathbf{x}}_p = \left[\hat{\mathbf{p}}_{\tilde{\mathbf{z}}};\ \hat{\mathbf{p}}_{\tilde{\mathbf{y}}};\ \hat{\mathbf{p}}_{\Delta\mathbf{v}};\ \hat{\mathbf{p}}_{\boldsymbol{\tau}};\ \hat{\mathbf{p}}_a\right] \tag{32}$$

**Rendezvous Navigation Filter Formulations**

Four specific relative navigation filter formations are investigated which include the 1) dual inertial, 2) chaser inertial relative, 3) target inertial relative and 4) the relative only filters. The specific number and type of states for each filter is defined along with the corresponding mapping matrix. Each of the formulations strive to replicate in complexity and scope the preliminary Orion translational relative navigation filter design for rendezvous, proximity operations, and docking [1].

For reference, the preliminary Orion translational relative navigation filter is a variant of the extended Kalman filter. It is composed of two inertial position and velocity states, one for Orion ($\hat{\mathbf{r}}_c$ and $\hat{\mathbf{v}}_c$) and one for the target vehicle ($\hat{\mathbf{r}}_t$ and $\hat{\mathbf{v}}_t$). Although the previous navigation architecture proposed having a separate relative attitude determination filter, an estimate of Orion's attitude $\hat{\mathbf{q}}_{\hat{c}}^{c}$ is still maintained in the translational filter along with various sensor misalignment and bias states. The number of filter states evolves depending on availability of sensor measurements. When a bearing measurement is available, the bearing sensor misalignment $\hat{\boldsymbol{\epsilon}}$ and bias states, $\hat{b}_\alpha$ and $\hat{b}_e$, are initialized. When range or range-rate measurements are provided, their corresponding biases, $\hat{b}_\rho$ and $\hat{b}_{\dot{\rho}}$, are included. As a result, the filter state vector contains a maximum of 22 elements.

$$\hat{\mathbf{x}}_{\text{Orion}} = \left[\hat{\mathbf{r}}_c;\ \hat{\mathbf{v}}_c;\ \hat{\mathbf{q}}_{\hat{c}}^{c} \mid \hat{\mathbf{r}}_t;\ \hat{\mathbf{v}}_t \mid \hat{\boldsymbol{\epsilon}};\ \hat{\mathbf{b}}\right] \tag{33}$$

**Dual Inertial Filter** The dual inertial (DI) formulation replicates most closely the original Orion relative navigation filter design. It maintains the chaser inertial position, velocity, and attitude states along with the target vehicle's inertial position and velocity. The parameter states include sensor misalignment and biases.

$$\hat{\mathbf{x}}_{DI} = \left[\hat{\mathbf{r}}_c;\ \hat{\mathbf{v}}_c;\ \hat{\mathbf{q}}_{\hat{c}}^{c} \mid \hat{\mathbf{r}}_t;\ \hat{\mathbf{v}}_t \mid \hat{\boldsymbol{\epsilon}};\ \hat{\mathbf{b}}\right] \tag{34}$$

The resulting mapping matrix $\hat{\mathbf{M}}_{DI}$ for the dual inertial filter formulation becomes,

$$\hat{\mathbf{M}}_{DI} = \left[\begin{array}{ccc|cccc|cccccc} \mathbf{I}_{r_c} & \mathbf{0}_{v_c} & \mathbf{0}_{q_c} & \mathbf{0}_{r_t} & \mathbf{0}_{v_t} & \mathbf{0}_{q_t} & \mathbf{0}_{w_t} & \mathbf{0} & \dots & \mathbf{0}_{\epsilon} & \mathbf{0}_{b} & \dots & \mathbf{0} \\ \mathbf{0}_{r_c} & \mathbf{I}_{v_c} & \mathbf{0}_{q_c} & \mathbf{0}_{r_t} & \mathbf{0}_{v_t} & \mathbf{0}_{q_t} & \mathbf{0}_{w_t} & \mathbf{0} & \dots & \mathbf{0}_{\epsilon} & \mathbf{0}_{b} & \dots & \mathbf{0} \\ \mathbf{0}_{r_c} & \mathbf{0}_{v_c} & \mathbf{I}_{q_c} & \mathbf{0}_{r_t} & \mathbf{0}_{v_t} & \mathbf{0}_{q_t} & \mathbf{0}_{w_t} & \mathbf{0} & \dots & \mathbf{0}_{\epsilon} & \mathbf{0}_{b} & \dots & \mathbf{0} \\ \hline \mathbf{0}_{r_c} & \mathbf{0}_{v_c} & \mathbf{0}_{q_c} & \mathbf{I}_{r_t} & \mathbf{0}_{v_t} & \mathbf{0}_{q_t} & \mathbf{0}_{w_t} & \mathbf{0} & \dots & \mathbf{0}_{\epsilon} & \mathbf{0}_{b} & \dots & \mathbf{0} \\ \mathbf{0}_{r_c} & \mathbf{0}_{v_c} & \mathbf{0}_{q_c} & \mathbf{0}_{r_t} & \mathbf{I}_{v_t} & \mathbf{0}_{q_t} & \mathbf{0}_{w_t} & \mathbf{0} & \dots & \mathbf{0}_{\epsilon} & \mathbf{0}_{b} & \dots & \mathbf{0} \\ \hline \mathbf{0}_{r_c} & \mathbf{0}_{v_c} & \mathbf{0}_{q_c} & \mathbf{0}_{r_t} & \mathbf{0}_{v_t} & \mathbf{0}_{q_t} & \mathbf{0}_{w_t} & \mathbf{0} & \dots & \mathbf{I}_{\epsilon} & \mathbf{0}_{b} & \dots & \mathbf{0} \\ \mathbf{0}_{r_c} & \mathbf{0}_{v_c} & \mathbf{0}_{q_c} & \mathbf{0}_{r_t} & \mathbf{0}_{v_t} & \mathbf{0}_{q_t} & \mathbf{0}_{w_t} & \mathbf{0} & \dots & \mathbf{0}_{\epsilon} & \mathbf{I}_{b} & \dots & \mathbf{0} \end{array}\right] \tag{35}$$

**Chaser Inertial Relative Filter** The chaser inertial relative (CIR) filter formulation preserves the inertial position, velocity, and attitude states of the chaser vehicle but replaces the target vehicle translational states with the relative position and velocity states, $\hat{\mathbf{r}}_r = \hat{\mathbf{r}}_t - \hat{\mathbf{r}}_c$ and $\hat{\mathbf{v}}_r = \hat{\mathbf{v}}_t - \hat{\mathbf{v}}_c$,

$$\hat{\mathbf{x}}_{CIR} = \left[\hat{\mathbf{r}}_c;\ \hat{\mathbf{v}}_c;\ \hat{\mathbf{q}}_{\hat{c}}^{c} \mid \hat{\mathbf{r}}_r;\ \hat{\mathbf{v}}_r \mid \hat{\boldsymbol{\epsilon}};\ \hat{\mathbf{b}}\right] \tag{36}$$

such that the corresponding filter formulation mapping matrix $\hat{\mathbf{M}}_{CIR}$ becomes,

$$\hat{\mathbf{M}}_{CIR} = \left[\begin{array}{ccc|cccc|cccccc} \mathbf{I}_{r_c} & \mathbf{0}_{v_c} & \mathbf{0}_{q_c} & \mathbf{0}_{r_t} & \mathbf{0}_{v_t} & \mathbf{0}_{q_t} & \mathbf{0}_{w_t} & \mathbf{0} & \dots & \mathbf{0}_{\epsilon} & \mathbf{0}_{b} & \dots & \mathbf{0} \\ \mathbf{0}_{r_c} & \mathbf{I}_{v_c} & \mathbf{0}_{q_c} & \mathbf{0}_{r_t} & \mathbf{0}_{v_t} & \mathbf{0}_{q_t} & \mathbf{0}_{w_t} & \mathbf{0} & \dots & \mathbf{0}_{\epsilon} & \mathbf{0}_{b} & \dots & \mathbf{0} \\ \mathbf{0}_{r_c} & \mathbf{0}_{v_c} & \mathbf{I}_{q_c} & \mathbf{0}_{r_t} & \mathbf{0}_{v_t} & \mathbf{0}_{q_t} & \mathbf{0}_{w_t} & \mathbf{0} & \dots & \mathbf{0}_{\epsilon} & \mathbf{0}_{b} & \dots & \mathbf{0} \\ \hline -\mathbf{I}_{r_c} & \mathbf{0}_{v_c} & \mathbf{0}_{q_c} & \mathbf{I}_{r_t} & \mathbf{0}_{v_t} & \mathbf{0}_{q_t} & \mathbf{0}_{w_t} & \mathbf{0} & \dots & \mathbf{0}_{\epsilon} & \mathbf{0}_{b} & \dots & \mathbf{0} \\ \mathbf{0}_{r_c} & -\mathbf{I}_{v_c} & \mathbf{0}_{q_c} & \mathbf{0}_{r_t} & \mathbf{I}_{v_t} & \mathbf{0}_{q_t} & \mathbf{0}_{w_t} & \mathbf{0} & \dots & \mathbf{0}_{\epsilon} & \mathbf{0}_{b} & \dots & \mathbf{0} \\ \hline \mathbf{0}_{r_c} & \mathbf{0}_{v_c} & \mathbf{0}_{q_c} & \mathbf{0}_{r_t} & \mathbf{0}_{v_t} & \mathbf{0}_{q_t} & \mathbf{0}_{w_t} & \mathbf{0} & \dots & \mathbf{I}_{\epsilon} & \mathbf{0}_{b} & \dots & \mathbf{0} \\ \mathbf{0}_{r_c} & \mathbf{0}_{v_c} & \mathbf{0}_{q_c} & \mathbf{0}_{r_t} & \mathbf{0}_{v_t} & \mathbf{0}_{q_t} & \mathbf{0}_{w_t} & \mathbf{0} & \dots & \mathbf{0}_{\epsilon} & \mathbf{I}_{b} & \dots & \mathbf{0} \end{array}\right] \tag{37}$$

**Target Inertial Relative Filter** The target inertial relative (TIR) filter formulation preserves the inertial position and velocity states of the target vehicle but replaces the chaser vehicle translational states with the relative position and velocity states, $\hat{\mathbf{r}}_r = \hat{\mathbf{r}}_t - \hat{\mathbf{r}}_c$ and $\hat{\mathbf{v}}_r = \hat{\mathbf{v}}_t - \hat{\mathbf{v}}_c$.

$$\hat{\mathbf{x}}_{_{TIR}} = \left[\hat{\mathbf{r}}_r;\ \hat{\mathbf{v}}_r;\ \hat{\mathbf{q}}_{\hat{c}}^{c} \mid \hat{\mathbf{r}}_t;\ \hat{\mathbf{v}}_t \mid \hat{\boldsymbol{\epsilon}};\ \hat{\mathbf{b}}\right] \tag{38}$$

The resulting filter formulation mapping matrix $\hat{\mathbf{M}}_{_{TIR}}$ for the target inertial relative design becomes,

$$\hat{\mathbf{M}}_{_{TIR}} = \left[\begin{array}{ccc|cccc|cccccc} -\mathbf{I}_{r_c} & \mathbf{0}_{v_c} & \mathbf{0}_{q_c} & \mathbf{I}_{r_t} & \mathbf{0}_{v_t} & \mathbf{0}_{q_t} & \mathbf{0}_{w_t} & \mathbf{0} & \dots & \mathbf{0}_{\epsilon} & \mathbf{0}_{b} & \dots & \mathbf{0} \\ \mathbf{0}_{r_c} & -\mathbf{I}_{v_c} & \mathbf{0}_{q_c} & \mathbf{0}_{r_t} & \mathbf{I}_{v_t} & \mathbf{0}_{q_t} & \mathbf{0}_{w_t} & \mathbf{0} & \dots & \mathbf{0}_{\epsilon} & \mathbf{0}_{b} & \dots & \mathbf{0} \\ \mathbf{0}_{r_c} & \mathbf{0}_{v_c} & \mathbf{I}_{q_c} & \mathbf{0}_{r_t} & \mathbf{0}_{v_t} & \mathbf{0}_{q_t} & \mathbf{0}_{w_t} & \mathbf{0} & \dots & \mathbf{0}_{\epsilon} & \mathbf{0}_{b} & \dots & \mathbf{0} \\ \hline \mathbf{0}_{r_c} & \mathbf{0}_{v_c} & \mathbf{0}_{q_c} & \mathbf{I}_{r_t} & \mathbf{0}_{v_t} & \mathbf{0}_{q_t} & \mathbf{0}_{w_t} & \mathbf{0} & \dots & \mathbf{0}_{\epsilon} & \mathbf{0}_{b} & \dots & \mathbf{0} \\ \mathbf{0}_{r_c} & \mathbf{0}_{v_c} & \mathbf{0}_{q_c} & \mathbf{0}_{r_t} & \mathbf{I}_{v_t} & \mathbf{0}_{q_t} & \mathbf{0}_{w_t} & \mathbf{0} & \dots & \mathbf{0}_{\epsilon} & \mathbf{0}_{b} & \dots & \mathbf{0} \\ \hline \mathbf{0}_{r_c} & \mathbf{0}_{v_c} & \mathbf{0}_{q_c} & \mathbf{0}_{r_t} & \mathbf{0}_{v_t} & \mathbf{0}_{q_t} & \mathbf{0}_{w_t} & \mathbf{0} & \dots & \mathbf{I}_{\epsilon} & \mathbf{0}_{b} & \dots & \mathbf{0} \\ \mathbf{0}_{r_c} & \mathbf{0}_{v_c} & \mathbf{0}_{q_c} & \mathbf{0}_{r_t} & \mathbf{0}_{v_t} & \mathbf{0}_{q_t} & \mathbf{0}_{w_t} & \mathbf{0} & \dots & \mathbf{0}_{\epsilon} & \mathbf{I}_{b} & \dots & \mathbf{0} \end{array}\right] \tag{39}$$

**Relative Only Filter** The relative only (RO) filter formulation replaces the inertial position and velocity states of both the chaser and target vehicles with the relative position and velocity states,

$$\hat{\mathbf{x}}_{_{RO}} = \left[\hat{\mathbf{r}}_r;\ \hat{\mathbf{v}}_r;\ \hat{\mathbf{q}}_{\hat{c}}^{c} \mid \hat{\boldsymbol{\epsilon}};\ \hat{\mathbf{b}}\right] \tag{40}$$

such that the corresponding filter formulation mapping matrix $\hat{\mathbf{M}}_{_{RO}}$ becomes

$$\hat{\mathbf{M}}_{_{RO}} = \left[\begin{array}{ccc|cccc|cccccc} -\mathbf{I}_{r_c} & \mathbf{0}_{v_c} & \mathbf{0}_{q_c} & \mathbf{I}_{r_t} & \mathbf{0}_{v_t} & \mathbf{0}_{q_t} & \mathbf{0}_{w_t} & \mathbf{0} & \dots & \mathbf{0}_{\epsilon} & \mathbf{0}_{b} & \dots & \mathbf{0} \\ \mathbf{0}_{r_c} & -\mathbf{I}_{v_c} & \mathbf{0}_{q_c} & \mathbf{0}_{r_t} & \mathbf{I}_{v_t} & \mathbf{0}_{q_t} & \mathbf{0}_{w_t} & \mathbf{0} & \dots & \mathbf{0}_{\epsilon} & \mathbf{0}_{b} & \dots & \mathbf{0} \\ \mathbf{0}_{r_c} & \mathbf{0}_{v_c} & \mathbf{I}_{q_c} & \mathbf{0}_{r_t} & \mathbf{0}_{v_t} & \mathbf{0}_{q_t} & \mathbf{0}_{w_t} & \mathbf{0} & \dots & \mathbf{0}_{\epsilon} & \mathbf{0}_{b} & \dots & \mathbf{0} \\ \hline \mathbf{0}_{r_c} & \mathbf{0}_{v_c} & \mathbf{0}_{q_c} & \mathbf{0}_{r_t} & \mathbf{0}_{v_t} & \mathbf{0}_{q_t} & \mathbf{0}_{w_t} & \mathbf{0} & \dots & \mathbf{I}_{\epsilon} & \mathbf{0}_{b} & \dots & \mathbf{0} \\ \mathbf{0}_{r_c} & \mathbf{0}_{v_c} & \mathbf{0}_{q_c} & \mathbf{0}_{r_t} & \mathbf{0}_{v_t} & \mathbf{0}_{q_t} & \mathbf{0}_{w_t} & \mathbf{0} & \dots & \mathbf{0}_{\epsilon} & \mathbf{I}_{b} & \dots & \mathbf{0} \end{array}\right] \tag{41}$$

## RELATIVE NAVIGATION FILTER PERFORMANCE RESULTS

Given the techniques to model and analyze various filter formulations, this section evaluates their performance in context of the EM-3 rendezvous scenarios introduced previously which include the co-manifested payload (CPL) extraction after the trans-lunar injection (TLI) burn and the rendezvous and docking with the deep space gateway (DSG) following insertion into the Earth/Moon near rectilinear halo orbit (NRHO). The key performance metrics to evaluate each filter formulation includes the navigation error for the 1) relative state, 2) chaser inertial state, and 3) target inertial state; along with the relative trajectory dispersions.

To properly compare the performance of each filter formulation, it is essential that the initialization of each filter is done consistently. In addition, several key trends and characteristics of the filter design depend on whether the chaser and target states of the initial covariance are correlated or not. Table 2 summarizes the two different approaches for initializing each filter assuming the chaser and target initial covariances, $\mathbf{P}_{cc}$ and $\mathbf{P}_{tt}$, are the same for each. The first column illustrates the initial covariance $\hat{\mathbf{P}}_{_{01}}$ assuming there are no correlations between the chaser and target states. For this case, the initial relative covariance is simply the sum of the chaser and target initial covariances, $\mathbf{P}_{r1} = \mathbf{P}_{cc} + \mathbf{P}_{tt}$. The second column summarizes the initial covariance $\hat{\mathbf{P}}_{_{02}}$ assuming there are correlations between the chaser and target states such that the cross correlation term is defined as $\mathbf{P}_{tc} = \mathbf{P}_{ct} = \frac{1}{2}(\mathbf{P}_{cc} + \mathbf{P}_{tt} - \mathbf{P}_{r2})$. For this circumstance, the relative navigation error is set to $\mathbf{P}_{r2} = \mathbf{P}_{tt} - \mathbf{P}_{cc}$ such that $\mathbf{P}_{tc} = \mathbf{P}_{cc}$. Each filter is evaluated for the two different initialization methods.

### Orion Proximity Operations, Docking, and Undocking at Post-TLI

The nominal transposition and docking profile for Orion during the post-TLI rendezvous and proximity operations is summarized in Figure 5. Figure 5(a) highlights the in-plane trajectory profile and Figure 5(b)

| Filter Formulation | Init Cov #1: No Correlation ($\hat{\mathbf{P}}_{01}$) | Init Cov #2: Correlation ($\hat{\mathbf{P}}_{02}$) |
|---|---|---|
| **1: Dual Inertial** | $\hat{\mathbf{M}}_{DI}\hat{\mathbf{P}}_{01}\hat{\mathbf{M}}_{DI}^{\mathrm{T}} = \begin{bmatrix} \mathbf{P}_{cc} & \mathbf{0} \\ \mathbf{0} & \mathbf{P}_{tt} \end{bmatrix}$ | $\hat{\mathbf{M}}_{DI}\hat{\mathbf{P}}_{02}\hat{\mathbf{M}}_{DI}^{\mathrm{T}} = \begin{bmatrix} \mathbf{P}_{cc} & \mathbf{P}_{tc} \\ \mathbf{P}_{ct} & \mathbf{P}_{tt} \end{bmatrix}$ |
| **2: Chaser Inertial Relative** | $\hat{\mathbf{M}}_{CIR}\hat{\mathbf{P}}_{0}\hat{\mathbf{M}}_{CIR}^{\mathrm{T}} = \begin{bmatrix} \mathbf{P}_{cc} & -\mathbf{P}_{cc} \\ -\mathbf{P}_{cc} & \mathbf{P}_{r1} \end{bmatrix}$ | $\hat{\mathbf{M}}_{CIR}\hat{\mathbf{P}}_{0}\hat{\mathbf{M}}_{CIR}^{\mathrm{T}} = \begin{bmatrix} \mathbf{P}_{cc} & \mathbf{0} \\ \mathbf{0} & \mathbf{P}_{r2} \end{bmatrix}$ |
| **3: Target Inertial Relative** | $\hat{\mathbf{M}}_{TIR}\hat{\mathbf{P}}_{0}\hat{\mathbf{M}}_{TIR}^{\mathrm{T}} = \begin{bmatrix} \mathbf{P}_{r1} & \mathbf{P}_{tt} \\ \mathbf{P}_{tt} & \mathbf{P}_{tt} \end{bmatrix}$ | $\hat{\mathbf{M}}_{TIR}\hat{\mathbf{P}}_{0}\hat{\mathbf{M}}_{TIR}^{\mathrm{T}} = \begin{bmatrix} \mathbf{P}_{r2} & \mathbf{0} \\ \mathbf{0} & \mathbf{P}_{tt} \end{bmatrix}$ |
| **4: Relative-Only** | $\hat{\mathbf{M}}_{RO}\hat{\mathbf{P}}_{0}\hat{\mathbf{M}}_{RO}^{\mathrm{T}} = \begin{bmatrix} \mathbf{P}_{r1} \end{bmatrix}$ | $\hat{\mathbf{M}}_{RO}\hat{\mathbf{P}}_{0}\hat{\mathbf{M}}_{RO}^{\mathrm{T}} = \begin{bmatrix} \mathbf{P}_{r2} \end{bmatrix}$ |

**Table 2. Onboard Filter Initial Covariance: With and Without Correlation Terms**

shows the nominal downrange, cross-track, and altitude profiles as a function of time. The total simulated duration from initial separation to extracting the CPL is approximately an hour. The sensors utilized include the rendezvous lidar, angle measurements to a set of target retro-reflectors [37], star tracker for attitude determination, gyros, and accelerometers.

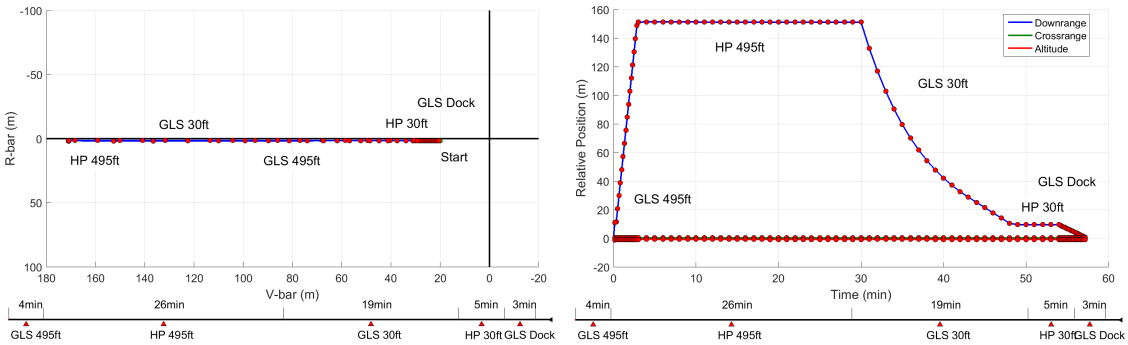


(a) Nominal Trajectory In-Plane

(b) Nominal Trajectory Time-History

**Figure 5. Post-TLI Transposition and Docking Nominal Relative Trajectory Profile**

The performance results for the four different filter formulations are provided in Figure 6. Since this scenario starts with Orion attached to the EUS/CPL, the target spacecraft; only the correlated initial condition scenarios are presented. For each sub-figure, the left plot emphasizes the dual inertial results and also indicates the sensor utilization schedule. The right plot shows the difference in performance between the dual inertial filter and the other formulation designs for comparison.

The relative navigation error for each filter design is summarized in Figure 6(a). For the transposition, docking, and extraction segment where the relative distance between the two vehicles remains within hundreds of feet and only relative sensors are utilized; the relative navigation performance for each filter formulation is the same. Not only are the processed measurements primarily from relative sensors, the targeting algorithms adopted are relative targeting algorithms. As a result, the relative trajectory dispersions in Figure 6(b) are also the same for each filter design. The inertial navigation position errors for both the chaser and target are included in Figure 6(c) and Figure 6(d) respectively. These plots highlight that the relative measurements with the Orion and target vehicle inertial states completely correlated, provides no additional inertial information as evident with the constantly increasing filter 3-sigma uncertainty bounds. Based on these metrics alone, there are no significant discriminators between the various formulation options.

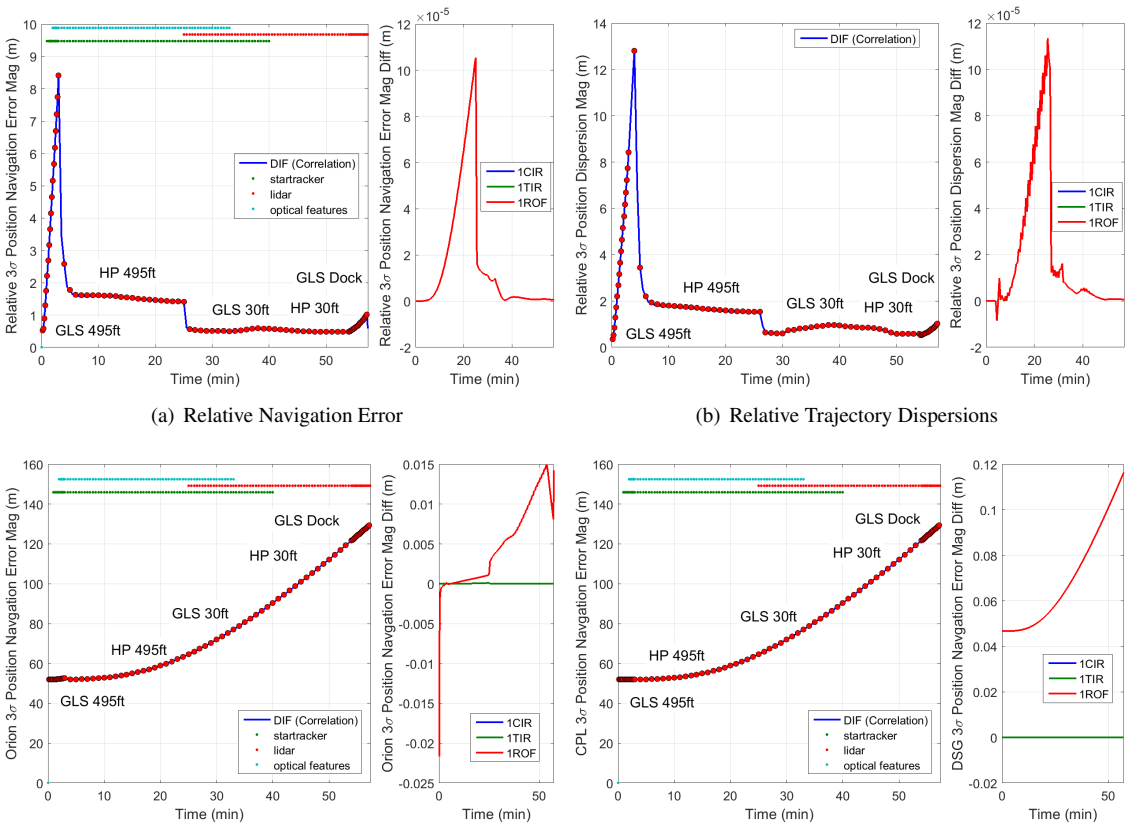


(a) Relative Navigation Error

(b) Relative Trajectory Dispersions

(c) Chaser Navigation Error

(d) Target Navigation Error

**Figure 6. Post-TLI Transposition and Docking Relative Filter Formulation Performance Results**

## Orion Proximity Operations and Docking at NRHO

The nominal trajectory profile for the notional close proximity operations and docking scenario with DSG in the NRHO is highlighted in Figure 7. It starts 15 minutes prior to the NRI burn such that the subsequent

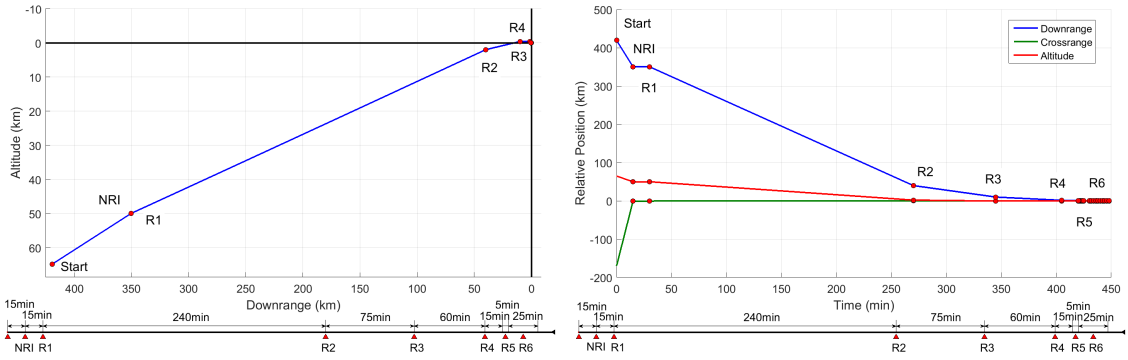


(a) Nominal Trajectory In-Plane

(b) Nominal Trajectory Time-History

**Figure 7. NRHO Nominal Relative Trajectory Profile**

rendezvous sequence takes a total of 7 hours to dock. The sensors utilized include an S-band range and range-rate measurements, star tracker bearing measurements, lidar, visible camera, accelerometers, gyros, and a

startracker for attitude estimation. The large NRI burn is computed with the Orion two-level targeter [38] and the subsequent rendezvous maneuvers utilize both inertial and relative targeting algorithms. The nominal in-plane trajectory is illustrated in Figure 7(a) with the relative downrange, cross-track, and altitude profiles as a function time summarized in Figure 7(b).

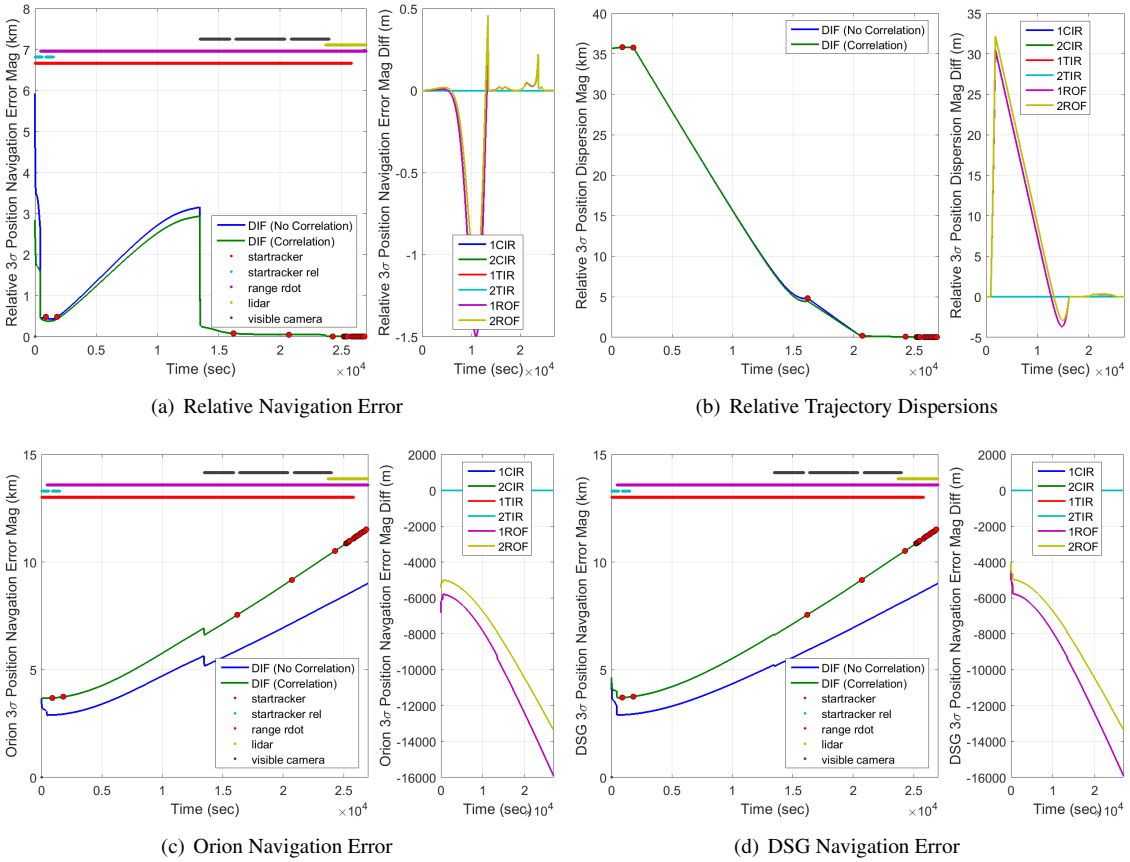


(a) Relative Navigation Error

(b) Relative Trajectory Dispersions

(c) Orion Navigation Error

(d) DSG Navigation Error

**Figure 8. NRHO Relative Filter Formulation Performance Results**

The resulting performance of each filter formulation (dual inertial, chaser inertial relative, target inertial relative, and relative-only) given initial navigation state errors that are both uncorrelated and correlated (labeled 1 and 2 respectively) for the NRHO rendezvous and docking sequence is provided in Figure 8. For each sub-figure, the left plot emphasizes the dual inertial results when the initial Orion and DSG navigation states are not correlated and correlated. It also highlights when each sensor is utilized. The right plot shows the difference in performance of the other filter formulations compared to the dual inertial to facilitate direct comparison of each design. The relative navigation errors are summarized in Figure 8(a) with the corresponding relative trajectory dispersions in Figure 8(b). The inertial navigation errors for both the chaser and target translational states is provided in Figure 8(c) and Figure 8(d) respectively.

During this flight phase, there are several key observations regarding the filter design that are noted. First, the dual inertial, chaser inertial relative, and target inertial relative have nearly identical performance results supporting the theoretical equivalence developed previously. Second, when the inertial position and velocity state vectors for Orion and DSG are correlated, Orion's inertial state estimate is largely unaffected by processing relative measurements. However, when the correlations are removed at initialization, the relative measurements cause both vehicle's inertial states to be updated indicating relative measurements provide inertial state information. Third, the relative-only filter has a degraded performance compared to the other formulations as anticipated, but from a relative navigation estimation aspect it differs only by several meters.

Since it is unable to accurately estimate the inertial states of both vehicles, the resulting relative trajectory dispersions due to both inertial targeting and navigation errors become much larger and are on the order of 30 meters (3-sigma) following the NRI maneuver. Noting the ratio between the navigation errors and trajectory dispersions in context of the separation distances, the relative-only filter formulation may still be sufficient.

## CONCLUSION

As rendezvous, proximity operations, and docking re-emerges into the Orion program, the relative navigation system will continue to be developed and analyzed to support NASA's exploration missions. A preliminary step has begun by re-evaluating the formulation of the translational relative navigation filter design. Various design options were introduced and analyzed both from a theoretical and flight heritage perspective along with simulation filter performance results based on the anticipated EM-3 mission RPOD scenarios. For the Orion program where the rendezvous flight domains will likely still include traditional environments such as low Earth orbit or low lunar orbit, new challenges are emerging as RPOD activities are envisioned in cis-lunar space to support assets in halo orbits in the Earth/Moon system. Given the expectation that both inertial and relative sensors along with inertial and relative guidance and targeting algorithms are necessary to support rendezvous and proximity operations; the dual inertial filter formulation was initially identified as the baseline approach. However, other formulations such as the target inertial relative or the chaser inertial relative have shown to possess comparable performance qualities but have other potential advantages related to the properties of the filter covariance. Other design factors may ultimately drive the particular formulation besides navigation and trajectory dispersion performance metrics.

## REFERENCES


[1] C. Hanak and C. D'Souza, "Preliminary Orion Command Module Translational Relative Navigation Filter Design for Rendezvous, Proximity Operations, and Docking, Rev.1," Tech. Rep. FltDyn-CEV-08-20, NASA, ISS Program, JSC, 2009.

[2] K. Hambleton, "Deep Space Gateway to Open Opportunities for Distant Destinations," *NASA*, 28 Mar 2017.

[3] J. Williams, D. E. Lee, R. J. Whitley, K. A. Bokelmann, D. C. Davis, and C. F. Berry, "Targeting cislunar near rectilinear halo orbits for human space exploration," in *American Astronautical Society*, pp. AAS 17–267, 1017.

[4] D. J. Grebow, M. T. Ozimek, K. C. Howell, and D. C. Folta, "Multibody orbit architectures for lunar south pole coverage," *Journal of Spacecraft and Rockets*, vol. 45, no. 2, March-April 2008.

[5] M. Gates, MikeBarrett, K. Schubert, and E. Lyon, "Power Propulsion Element For Deep Space Gateway Concept: Request for Information and Synopsis Virtual Industry Forum," *NASA*, 24 July 2017.

[6] F. D. Clark, P. T. Spehar, J. P. Brazzel Jr, and H. D. Hinkel, "Laser-based relative navigation and guidance for space shuttle proximity operations," 2003.

[7] K. Mand, "Rendezvous and Proximity Operations at the Earth-Moon L2 Lagrange Point: Navigation Analysis for Preliminary Trajectory Design," Master's thesis, Rice University, May 2014.

[8] H. D. Curtis, *Orbital mechanics for engineering students*. Butterworth-Heinemann, 2013.

[9] G. Gaias, S. D'Amico, and J.-S. Ardaens, "Angles-only navigation to a noncooperative satellite using relative orbital elements," *Journal of Guidance, Control, and Dynamics*, 2014.

[10] E. S. Muller and P. M. Kachmar, "A new approach to on-board orbit navigation," *Navigation*, vol. 18, no. 4, pp. 369–385, 1971.

[11] M. L. Psiaki, "Autonomous orbit determination for two spacecraft from relative position measurements," *Journal of Guidance Control and Dynamics*, vol. 22, pp. 305–312, 1999.

[12] S. Jenkins and D. Geller, "State estimation and targeting for autonomous rendezvous and proximity operations (aas 07-316)," *ADVANCES IN THE ASTRONAUTICAL SCIENCES*, vol. 129, no. 2, p. 1071, 2008.

[13] E. S. Muller and P. M. Kachmar, *The Apollo Rendezvous Navigation Filter Theory, Description and Performance*. MIT Charles Stark Draper Laboratory, 1970.

[14] I. R. Frame, "History of space shuttle rendezvous and proximity operations," *Journal of Spacecraft and Rockets*, vol. 43, no. 5, 2006.

[15] I. Mitchell, T. Gorton, K. Taskov, M. Drews, R. Luckey, M. Osborne, L. Page, H. Norris, and S. Shepperd, "Gn&c development of the xss-11 micro-satellite for autonomous rendezvous and proximity operations," in *29th Annual AAS Guidance and Control Conference*, pp. 1–17, 2006.

[16] P. S. Maybeck, *Stochastic models, estimation, and control*, vol. 1. New York: Academic Press, 1979.

[17] D. K. Geller, "Linear Covariance Techniques for Orbital Rendezvous Analysis and Autonomous Onboard Mission Planning," *Journal of Guidance, Control, and Dynamics*, vol. 29, pp. 1404–1414, November-December 2006.

[18] D. C. Woffinden and D. K. Geller, "Relative Angles-Only Navigation and Pose Estimation for Autonomous Orbital Rendezvous," *Journal of Guidance, Control, and Dynamics*, vol. 30, pp. 1455–1469, September-October 2007.

[19] C. D'Souza and et. al., "Orion rendezvous, proximity operations, and docking design and analysis," in *AIAA 2007-6683*, 2007.

[20] C. N. D'Souza, F. C. Hanak, P. Spehar, F. D. Clark, and M. Jackson, "Orion Cislunar Guidance and Navigation," in *AIAA Guidance, Navigation, and Control (GNC) Conference*, (Hilton Head, SC), AIAA 2007-6681, 20-23 August 2007.

[21] P. Miotto, L. Breger, I. Mitchell, B. Keller, and B. Rishikof, "Designing and validating proximity operations rendezvous and approach trajectories for the cygnus mission," in *AIAA 2010-8446*, 2010.

[22] D. Woffinden, L. Epstein, G. Stafford, T. Mosher, J. Curry, and Z. Krevor, "Dream chaser on-orbit operations: Preliminary trajectory design and analysis," in *AIAA Guidance, Navigation, and Control (GNC) Conference*, (Portand, OR), AIAA 2011-6654, 8-11 August 2011.

[23] R. Zanetti, D. C. Woffinden, and A. Sievers, "Multiple Event Triggers in Linear Covariance Analysis for Spacecraft Rendezvous," *Jounral of Guidance, Control, and Dynamics*, vol. 35, pp. 353–366, March-April 2012.

[24] M. Osenar, F. Clark, and C. D'Souza, "Performance of an Automated Feature Tracking Lunar Navigation System," in *AAS/AIAA Space Flight Mechanic Meeting*, (Galveston, TX), AAS 08-101, 27-31 January 2008.

[25] N. B. Stastny and D. K. Geller, "Autonomous optical navigation at jupiter: A linear covariance analysis," *Journal of Spacecraft and Rockets*, vol. 45, pp. 974–981, Mar-Apr 2008.

[26] D. Geller and D. Christensen, "Linear Covariance Analysis for Powered Lunar Descent and Landing," *The Journal of Spacecraft and Rockets*, vol. 46, pp. 1231–1248, Nov-Dec 2009.

[27] D. Geller, "Analysis of the relative attitude estimation and control problem for satellite inspection and orbital rendezvous," *The Journal of the Astronautical Sciences*, vol. 55, pp. 195–214, June 2007.

[28] T. J. Moesser and D. K. Geller, "Guidance and navigation linear covariance analysis for lunar powered descent," in *AAS/AIAA Astrodynamics Specialist Conference*, (Mackinac Island, Michigan), AAS 07-313, August 2007.

[29] M. B. Rose and D. K. Geller, "Linear covariance techniques for powered ascent," in *AIAA 2010-8175*, 2010.

[30] C. D'Souza and F. Clark, "Linear covariance analysis techniques applied to orion cislunar operations," in *AIAA and AAS Space Flight Mechanics Conference*, (Galveston, TX), AAS 08-100, 27-31 January 2008.

[31] R. Zanetti, "Autonomous Midcourse Navigation for Lunar Return," *Jounral of Spacecraft and Rockets*, vol. 46, pp. 865–873, July-Aug 2009.

[32] C. D'Souza and R. Zanetti, "Navigation and dispersion analysis of the first orion exploration mission," in *AAS/AIAA Astrodynamics Specialist Conference*, (Vail, CO), AAS 15-768, 9-13 Aug 2015.

[33] C. D'Souza and R. Zanetti, "Navigation design and analysis for the orion exploration mission 2," in *AAS/AIAA Astrodynamics Specialist Conference*, (Stevenson, WA), AAS 17-643, 20-24 Aug 2017.

[34] D. Woffinden and L. Breger, "Automated Derivation and Verification of Navigation Requirements for On-orbit Rendezvous," in *AIAA Guidance, Navigation, and Control (GNC) Conference*, (Boston, MA), AIAA 2013-4964, 19-22 August 2013.

[35] K. Mand, D. Woffinden, P. Spanos, and R. Zanetti, "Rendezvous and Proximity Operations at the Earth-Moon L2 Lagrange Point: Navigation Analysis for Preliminary Trajectory Design," in *AAS/AIAA Space Flight Mechanic Meeting*, (Santa Fe, New Mexico), AAS 14-376, 26-30 January 2014.

[36] D. Woffinden, S. Bhatt, and D. Kirkpatrick, "Optimal multi-variable multi-constraint spacecraft gn&c requirement derivation," *AAS Guidance and Control Conference*, vol. AAS 18-095, 2-7 Feb 2018.

[37] S. Robinson, C. Ertl, and J. Christian, "Retro-reflector pattern design and identification for orion rendezvous, proximity operations, and docking," *AAS Guidance and Control Conference*, vol. AAS 18-143, 2 - 7 Feb 2018.

[38] S. Scarritt, T. Fill, and S. Robinson, "Advances in orion's on-orbit guidance and targeting system architecture," *AAS Guidance and Control Conference*, vol. AAS 15-096, 30 Jan - 4 Feb 2015.

# Information Formulation of the UDU Kalman Filter

Christopher D'Souza and Renato Zanetti

***Abstract*—A new information formulation of the Kalman filter is presented where the information matrix is parameterized as the product of an upper triangular matrix, a diagonal matrix, and the transpose of the triangular matrix (UDU factorization). The UDU factorization of the Kalman filter is known for its numerical stability, this work extends the technique the information filter. A distinct characteristic of the new algorithm is that measurements can be processed as vectors, while the classic UDU factorization requires scalar measurement processing, i.e. a diagonal measurement noise covariance matrix.**

## I. Introduction

The UDU formulation of the Kalman Filter has been used in aerospace engineering applications for several decades. Thornton[1], Bierman and Thornton [2] and Bierman [3] introduced an elegant formulation where the covariance matrix $P$ is replaced by two factors: a diagonal matrix $D$ and an upper triangular matrix $U$ with ones on the main diagonal, such that $P = UDU^T$. Whereas the UDU factorization improves the computational stability and efficiency of large navigation filters, it was originally used in a batch formulation [4]. However, this formulation lent itself to sequential implementations, well-suited for platforms where both computational stability and numerical efficiency are at a premium. It serves as the backbone of the Orion Navigation System [5].

Factorization of the covariance matrix in a Kalman filter [6] is almost as old as the filter itself. In 1963 James Potter developed a square-root formulation of the Kalman filter to implement on the Apollo onboard computer[7]. The main driver at the time was numerical precision, as computer words were only 8 bits long. Replacing the covariance by a square root matrix $S$, such as $P = SS^T$, reduces the spread of the elements of $P$ bringing them closer to 1, doubling the numerical precision of the stored variable. Potter's algorithm requires the computation of scalar square roots (one per measurement). At the time, the Apollo Kalman filter was designed without any process noise, because computations required for inclusion of the process noise required too many computations[8]. A very desirable by-product of this factorization is that the symmetry and semi-positive definiteness of the covariance are insured by construction, and does not need to be checked or enforced to correct for numerical and round-off errors. It should be noted that this Apollo factorization was not a triangular square root matrix.

An alternative square root covariance factorization is the Cholesky factorization [9], [10]. The Cholesky method is very similar to Potter's but computes the square root of the covariance matrix with a Cholesky decomposition ($S$ is a triangular matrix)[11]. Another relevant covariance factorization work is that proposed by Oshman and Bar-Itzhack [12], which utilizes the spectral decomposition of the covariance matrix.

The UDU factorization is not a square root filter; the numerical precision of the stored variable does not increase due to the factorization. For example, if $P$ is diagonal, $U = I$ and $D = P$; therefore the full range of values in $P$ are preserved in this factorization. However, the $UDU$ formulation of the Kalman filter has great numerical stability properties [3]; it insures symmetry of the covariance by construction, and it requires a trivial check and correction to ensure semi-positive definiteness (it suffices to enforce that the diagonal elements of $D$ remain non-negative). The UDU formulation is free from square root operations, making it computationally cheaper than the Cholesky approach. For these reasons the UDU has endured as one of the preferred practical implementation of Kalman filters in aerospace applications.

While the UDU factorization is well known, it has never been applied to the information formulation of the Kalman filter [13], [14], [15]. In this formulation the inverse of the covariance matrix, known as the information matrix, is carried in the recursive algorithm rather than the covariance matrix itself. The information formulation is a popular approach in several situations. In particular, the Square Root Information Filter (SRIF) [16], [17], [18], [3], [19], [20] is a go-to Kalman filter factorization method used in orbit determination packages such as Monte because of its great stability and accuracy. In this work we introduce the UDU Information Filter, a never developed before algorithm with two key properties that make it a very desirable implementation of a recursive estimator: i. unlike the regular UDU filter, measurements do not need to be processed as scalars, i.e. the measurement noise covariance matrix $R$ does not need to be diagonal or diagonalized, and ii. unlike the regular information formulation the state estimation error covariance matrix does not actually need to be inverted.

## II. Background

The well-known Kalman filter equations measurement update equation are given by

$$\hat{\mathbf{x}}_k = \bar{\mathbf{x}}_k + K_k(\mathbf{y}_k - H_k\bar{\mathbf{x}}_k) \tag{1}$$

$$\begin{aligned} P_k &= \bar{P}_k - \bar{P}_k H_k^T (H_k \bar{P}_k H_k^T + R_k)^{-1} H_k \bar{P}_k \\ &= (I - K_k H_k)\, \bar{P}_k \end{aligned} \tag{2}$$

$$K_k = \bar{P}_k H_k^T (H_k \bar{P}_k H_k^T + R_k)^{-1} \;=\; P_k H_k^T R_k^{-1} \tag{3}$$

where the bar represent the *a priori* value, $K_k$ is the $n \times m$ Kalman gain, $\mathbf{x} \in \Re^n$ is the state vector, $P_k$ is the $n \times n$ es-

C. D'Souza is with the Aeroscience and Flight Mechanics Division, EG6, 2101 NASA Parkway, NASA Johnson Space Center, Houston, Texas 77058.

Renato Zanetti is with the Department of Aerospace Engineering and Engineering Mechanics, The University of Texas at Austin, Austin, Texas 78712

timation error covariance matrix, $\mathbf{y} \in \Re^m$ is the measurement vector defined as

$$\mathbf{y}_k = H_k \mathbf{x}_k + \boldsymbol{\eta}_k \tag{4}$$

where $\boldsymbol{\eta}_k$ is a zero mean, white sequence with covariance matrix $R_k$. The propagation equations are

$$\bar{\mathbf{x}}_{k+1} = \Phi(t_{k+1}, t_k)\hat{\mathbf{x}}_k \tag{5}$$

$$\begin{aligned}\bar{P}_{k+1} &= \Phi(t_{k+1}, t_k) P_k \Phi(t_{k+1}, t_k)^T + G_k Q_k G_k^T \\ &= \Phi_k P_k \Phi_k^T + G_k Q_k G_k^T\end{aligned} \tag{6}$$

where $\Phi(t_{k+1}, t_k)$ (which we will denote as $\Phi_k$) is the state $n \times n$ transition matrix from $t_{k-1}$ to $t_k$, $Q_k$ is the $p \times p$ process noise covariance matrix, and $G_k$ is the $n \times p$ process noise shaping matrix.

The UDU factorization implements the above equations by replacing the covariance matrix $P_k$ with an upper triangular matrix with ones on the diagonal ($U_k$) and a diagonal matrix $D_k$, such that

$$P_k = U_k D_k U_k^T \tag{7}$$

The UDU approach to propagate $U_k$ and $D_k$ forward in time makes use of the Modified Weighted Gram-Schmidt (MWGS) orthogonalization algorithm that avoids loss of orthogonality due to round-off errors [21]. Measurements are processed one at the time as scalars by noting that when $R_k$ is diagonal Eq. (2) the update is obtained by recursively processing one element of $\mathbf{y}_k$ at a time, using the corresponding row of $H_k$ and diagonal element of $R_k$. The measurement residual covariance matrix $W_k = H_k \bar{P}_k H_k^T + R_k$ thus becomes a scalar, and the quantity $\bar{P}_k H_k^T = \mathbf{w}_k$ becomes a vector; thus each of the scalar updates takes the form

$$P_k = \bar{P}_k - \frac{1}{W_k}\mathbf{w}_k \mathbf{w}_k^T \tag{8}$$

since matrix $\bar{P}_k$ is updated with a rank one matrix ($\frac{1}{W_k}\mathbf{w}_k\mathbf{w}_k^T$), we call this a rank one update, Agee and Turner [22] detailed how to directly update the $U_k$ and $D_k$ factors due to a rank one update. The subtraction in Eq. (8) could cause some numerical instabilities in Agee-Turner's algorithm. Carlson [23] introduced an alternative rank-one update algorithm that, while less generic, is more stable for the measurement update. Carlson's rank-one update is not valid for generic values of $\mathbf{w}_k$ and $W_k$, but only when the update is done with the optimal Kalman gain.

An alternative formulation of the Kalman filter is the information formulation, where the covariance matrix $P$ is replaced by its inverse. The covariance update and Kalman gain are calculated as

$$P_k^{-1} = \bar{P}_k^{-1} + H_k^T R_k^{-1} H_k \tag{9}$$

$$K_k = P_k H_k^T R_k^{-1} \tag{10}$$

The information formulation is particularly useful when there is no prior information, i.e. $P_0 = \infty$, in this case the covariance formulation of the KF is not defined, while the information formulation is, and starts from $P_0^{-1} = O$. In the covariance formulation, the $m \times m$ measurement residual covariance matrix $W_k = H_k \bar{P}_k H_k^T + R_k$ is inverted to process the measurement, while in the information formulation the $n \times n$ covariance matrix is inverted in the time propagation step. In situations when $m > n$, therefore, the information formulation could be computationally cheaper, although measurements are often processed one at the time as scalars. Processing measurements as scalars is only possible when $R$ is diagonal, otherwise the additional steps of a change of variables to diagonalize $R$ is required.

## III. The UDU Information Filter

### A. The Measurement Update

Begin with factoring the covariance $P$ into an LDL form; that is, rather than using an upper triangular matrix we will use a lower triangular matrix. We denote the diagonal matrix with $\Delta$

$$P_k \;=\; L_k\, \Delta_k\, L_k^T \quad \text{and} \quad \overline{P}_k \;=\; \overline{L}_k\, \overline{\Delta}_k\, \overline{L}_k^T \tag{11}$$

and we define $U$ and $D$ as the inverses of $L^T$ and $\Delta$, respectively

$$P_k^{-1} \;=\; L_k^{-T}\, \Delta_k^{-1}\, L_k^{-1} =\; U_k\, D_k\, U_k^T \tag{12}$$

$$\overline{P}_k^{-1} \;=\; \overline{L}_k^{-T}\, \overline{\Delta}_k^{-1}\, \overline{L}_k^{-1} =\; \overline{U}_k\, \overline{D}_k\, \overline{U}_k^T \tag{13}$$

so that the measurement update (Eq. (9)) becomes

$$U_k D_k U_k^T \;=\; \overline{U}_k \overline{D}_k \overline{U}_k^T + H_k^T R_k^{-1} H_k \tag{14}$$

We now factor the $m \times m$ matrix $R_k$ into LDL form as

$$R_k = L_{R_k} \Delta_{R_k} L_{R_k}^T \tag{15}$$

and

$$R_k^{-1} = L_{R_k}^{-T} \Delta_{R_k}^{-1} L_{R_k}^{-1} = U_{R_k} D_{R_k} U_{R_k}^T \tag{16}$$

so that Eq. (14) becomes

$$U_R D_R U_R^T \;=\; \overline{U}_R \overline{D}_R \overline{U}_R^T + H_R^T U_{R_k} D_{R_k} U_{R_k}^T H_R \tag{17}$$

We now work on the term $U_{R_k} H$ where we note that it is of dimension $m \times n$ so that it can be expressed as

$$U_{R_k}^T H_R \;=\; \begin{bmatrix} \mathbf{v}_1^T \\ \mathbf{v}_2^T \\ \vdots \\ \mathbf{v}_m^T \end{bmatrix} \tag{18}$$

where each $\mathbf{v}_i$ is an $n \times 1$ vector.

The factor $H_k^T R_k^{-1} H_k$ can be expressed as

$$\begin{aligned} H_k^T R_k^{-1} H_k &= H_k^T U_{R_k} D_{R_k} U_{R_k}^T H_k \\ &= \begin{bmatrix} \mathbf{v}_1^T \\ \mathbf{v}_2^T \\ \vdots \\ \mathbf{v}_m^T \end{bmatrix}^T \begin{bmatrix} 1/d_{1_R} & 0 & \cdots & 0 \\ 0 & 1/d_{2_R} & \cdots & 0 \\ \vdots & \vdots & \ddots & \vdots \\ 0 & 0 & \cdots & 1/d_{m_R} \end{bmatrix} \begin{bmatrix} \mathbf{v}_1^T \\ \mathbf{v}_2^T \\ \vdots \\ \mathbf{v}_m^T \end{bmatrix} \\ &= \sum_{i=1}^{m} \frac{1}{d_{i_R}} \mathbf{v}_i \mathbf{v}_i^T \end{aligned} \tag{19}$$

so that the measurement update equation is now

$$U_k D_k U_k^T \;=\; \overline{U}_k \overline{D}_k \overline{U}_k^T + \sum_{i=1}^{m} \frac{1}{d_{i_R}} \mathbf{v}_i \mathbf{v}_i^T \tag{20}$$

Thus it reduces to a series of $m$ rank-one updates.

Notice that Eq. (20) is the update equation due to a vector measurement so that the need to process scalar measurements, as in the covariance UDU formulation, is avoided in the proposed information UDU formulation. Rather than performing an eigenvalue decomposition of $R_k$ and a corresponding change of variables for $\mathbf{y}_k$, we simply perform the $UDU$ factorization of $R_k^{-1}$.

As stated earlier, one of the benefits of using an information formulation is that if $P_0$ is singular, this allows for an estimate to be obtained [14]. To this end, $\hat{\mathbf{z}}_k$ and $\bar{\mathbf{z}}_k$, which are directly related to $\hat{\mathbf{x}}_k$ and $\bar{\mathbf{x}}_k$, are defined as

$$\hat{\mathbf{z}}_k \triangleq P_k^{-1}\hat{\mathbf{x}}_k\,, \qquad \bar{\mathbf{z}}_k \triangleq P_k^{-1}\bar{\mathbf{x}}_k \tag{21}$$

Premultiplying Eq. (1) by $P_k^{-1}$, we get

$$\begin{aligned}\hat{\mathbf{z}}_k &= P_k^{-1}\left(I - K_k H_k\right)\bar{\mathbf{x}}_k + P_k^{-1}K_k\mathbf{y}_k &(22)\\ &= \bar{\mathbf{z}}_k + H_k R_k^{-1}\mathbf{y}_k &(23)\end{aligned}$$

### *B. The Time Update*

Prior to propagation, the standard information formulation of the Kalman filter inverts the information matrix to obtain the covariance, it then propagates the covariance with Eq. (6), and finally inverted the propagated covariance matrix to prepare for the measurement update phase. We propose an algorithm that propagates the factors of the information matrix directly. Starting from the covariance propagation Eq. (6), we factorize $Q_k$ via a UDU parameterization so that

$$Q_k = U_{Q_k}\,\Delta_{Q_k} U_{Q_k}^T \tag{24}$$

where $\Delta_{Q_k}$ is a diagonal $p \times p$ matrix and define $G_{Q_k}$ as

$$G_{Q_k} \triangleq G_k\,U_{Q_k} \tag{25}$$

so that $\overline{P}_k$ becomes

$$\overline{P}_{k+1} = \Phi_k\,P_k\,\Phi_k^T + G_{Q_k}\,\Delta_{Q_k}\,G_{Q_k}^T \tag{26}$$

Invoking the matrix inversion lemma

$$\left(Z + XAY\right)^{-1} = Z^{-1} - Z^{-1}X\left(A^{-1} + Y\,Z^{-1}X\right)^{-1}YZ^{-1} \tag{27}$$

and letting

$$Z = \Phi_k\,P_k\,\Phi_k^T; \quad A = \Delta_{Q_k}; \quad X = G_{Q_k}; \quad Y = G_{Q_k}^T \tag{28}$$

and

$$Z^{-1} = M_k \triangleq \Phi_k^{-T}\,P_k^{-1}\,\Phi_k^{-1} \tag{29}$$

The inverse of the propagated covariance is

$$\overline{P}_{k+1}^{-1} = M_k - M_k\,G_{Q_k}\left[G_k^T\,M_k\,G_{Q_k} + \Delta_{Q_k}^{-1}\right]^{-1}G_{Q_k}^T M_k \tag{30}$$

Defining

$$\overline{G}_k \triangleq \Phi_k^{-1}\,G_{Q_k} \qquad D_{Q_k} = \Delta_{Q_k}^{-1} \tag{31}$$

$P_{k+1}^{-1}$ becomes

$$\overline{P}_{k+1}^{-1} = \Phi_k^{-T}\Big\{P_k^{-1} - P_k^{-1}\,\overline{G}_k\left[\overline{G}_k^T\,P_k^{-1}\,\overline{G}_k + D_{Q_k}\right]^{-1}\overline{G}_k^T P_k^{-1}\Big\}\Phi_k^{-1} \tag{32}$$

and defining $\mathcal{K}_k$ as

$$\mathcal{K}_k \triangleq P_k^{-1}\,\overline{G}_k\left[\overline{G}_k^T\,P_k^{-1}\,\overline{G}_k + D_{Q_k}\right]^{-1} \tag{33}$$

Defining the quantity inside the brackets in Eq. (32) as $\mathcal{P}_k^{-1}$

$$\begin{aligned}\mathcal{P}_k^{-1} &\triangleq P_k^{-1} - P_k^{-1}\,\overline{G}_k\left[\overline{G}_k^T\,P_k^{-1}\,\overline{G}_k + D_{Q_k}\right]^{-1}\overline{G}_k^T P_k^{-1}\\ &= \left[I - \mathcal{K}_k\overline{G}_k^T\right]P_k^{-1} &(34)\end{aligned}$$

We notice Eq. (34) is an analog to Eq. (2) with

$$\begin{array}{lll}\mathcal{P}_k^{-1} \to P_k & \overline{G}_k \to H_k^T & D_{Q_k} \to R_k\\ P_k^{-1} \to \bar{P}_k & \mathcal{K}_k \to K_k & \end{array}$$

and since $D_{Q_k}$ is a diagonal $p \times p$ matrix, we can solve for the UDU factorization of $\mathcal{P}_k^{-1}$ directly by using a Carlson Rank-One Update [23] performed $p$ times on

$$\mathcal{U}_k\mathcal{D}_k\mathcal{U}_k^T = U_kD_kU_k^T - U_kD_kU_k^T\,\overline{G}_k\left[\overline{G}_k^T\,U_kD_kU_k^T\,\overline{G}_k + \Delta_{Q_k}^{-1}\right]^{-1}\overline{G}_k^T U_kD_kU_k \tag{35}$$

so that we can find the time-propagated UDU factors of $\overline{P}_k^{-1}$ as

$$\overline{P}_{k+1}^{-1} = \overline{U}_{k+1}\overline{D}_{k+1}\overline{U}_{k+1}^T = \Phi_k^{-T}\,\mathcal{U}_k\mathcal{D}_k\mathcal{U}_k^T\Phi_k^{-1} \tag{36}$$

Since this equation is equivalent to a covariance propagation without process noise, the MWGS orthogonalization algorithm can be used to obtain the factors $\overline{U}_{k+1}$ and $\overline{D}_{k+1}$.

Notice that $\Phi_k^{-1}$ does not necessarily need to be computed by a direct matrix inversion. Usually $\Phi_k$ is computed via integration of a matrix differential equation or by series approximation. Similarly, $\Phi_k^{-1}$ can be obtained directly by backwards integration or by series approximation.

Beginning with Eq. (5) the time update for $\bar{\mathbf{z}}_{k+1}$ is obtained as follows

$$\bar{P}_{k+1}^{-1}\bar{\mathbf{x}}_{k+1} = \bar{P}_{k+1}^{-1}\Phi_k\,P_k\,P_k^{-1}\hat{\mathbf{x}}_k \tag{37}$$

which becomes

$$\bar{\mathbf{z}}_{k+1} = \bar{P}_{k+1}^{-1}\Phi_k\,P_k\,\hat{\mathbf{z}}_k \tag{38}$$

substituting from Eqs. (32) and (34)

$$\bar{\mathbf{z}}_{k+1} = \Phi_k^{-T}\left[I - \mathcal{K}_k\overline{G}_k^T\right]\hat{\mathbf{z}}_k \tag{39}$$

or

$$\bar{\mathbf{z}}_{k+1} = \Phi^{-T}(t_{k+1}, t_k)\left[I - \mathcal{K}_k\overline{G}_k^T\right]\hat{\mathbf{z}}_k \tag{40}$$

### C. An Efficient Algorithm to compute $U^{-1}$

The algorithm proposed does not necessitate to invert the covariance matrix nor its $U$ or $L$ factor. However, in case the initial covariance was provided, it might be convenient to factorize it first, and to efficiently invert its factors rather than inverting the full covariance. In this section we compute the inverse in an efficient manner, taking advantage of the '1's' and '0's'. It is as follows: Given an $n \times n$ upper triangular 'unit' matrix $U$ expressed as

$$U = \begin{bmatrix} 1 & U_{1,2} & U_{1,3} & \cdots & U_{1,n-1} & U_{1,n} \\ 0 & 1 & U_{2,3} & \cdots & U_{2,n-1} & U_{2,n} \\ 0 & 0 & 1 & \cdots & U_{3,n-1} & U_{3,n} \\ \vdots & \vdots & \vdots & \ddots & \vdots & \vdots \\ 0 & 0 & 0 & \cdots & 1 & U_{n-1,n} \\ 0 & 0 & 0 & \cdots & 0 & 1 \end{bmatrix} \tag{41}$$

the inverse is also an $n \times n$ upper triangular 'unit' matrix $V$ (so that $\det(V) = 1$) which is

$$V = U^{-1} = \begin{bmatrix} 1 & V_{1,2} & V_{1,3} & \cdots & V_{1,n-1} & V_{1,n} \\ 0 & 1 & V_{2,3} & \cdots & V_{2,n-1} & V_{2,n} \\ 0 & 0 & 1 & \cdots & V_{3,n-1} & V_{3,n} \\ \vdots & \vdots & \vdots & \ddots & \vdots & \vdots \\ 0 & 0 & 0 & \cdots & 1 & V_{n-1,n} \\ 0 & 0 & 0 & \cdots & 0 & 1 \end{bmatrix} \tag{42}$$

since

$$U\,V \;=\; I \tag{43}$$

we can solve for the elements of $V$ as

$$\begin{aligned} j &= n-1, \cdots, 2, \qquad i = j-1, \cdots, 1 \\ V(i,j) &= -\left[ U(i,j) + \sum_{k=i+1}^{j-1} U(i,k) V(k,j) \right] \end{aligned} \tag{44}$$

## IV. A Numerical Example

In this section we show the performance of the algorithm in linear, time-varying example with correlated measurement noise covariance matrix $R$. The system is given by

$$\mathbf{x}_{k+1} = \Phi_k \mathbf{x}_k + \boldsymbol{\nu}_k \tag{45}$$

$$\mathbf{y}_k = H_k \mathbf{x}_k + \boldsymbol{\eta}_k \tag{46}$$

$$\Phi_k = \begin{bmatrix} I & A_k \\ B_k & I \end{bmatrix} \tag{47}$$

$$A_k = \begin{bmatrix} t_k & 0 \\ 0 & t_k \end{bmatrix} \tag{48}$$

$$B_k = 0.1 \begin{bmatrix} (\sin(t_k) - \sin(t_{k-1}) & -(\cos(t_k) - \cos(t_{k-1}) \\ 0 & (\sin(t_k) - \sin(t_{k-1}) \end{bmatrix} \tag{49}$$

$$H_k = \begin{bmatrix} 1 & 0 & 0 & 0 \\ 0 & 1 & 0 & 0 \end{bmatrix} \tag{50}$$

where $I$ is the identity matrix, $O$ the zero matrix, $t_k - t_{k-1} = 1$ second, $\boldsymbol{\nu}_k$ is a zero mean, Gaussian white sequence with covariance matrix $Q_k = 0.01\ I$, and $\boldsymbol{\eta}_k$ is a zero mean, Gaussian white sequence with covariance matrix $R_k$

$$R_k = \begin{bmatrix} 2.96 & 2.8 \\ 2.8 & 2.96 \end{bmatrix} \tag{51}$$

The initial estimate is unbiased, and the initial estimation error is Gaussian with covariance $P_0 = I$. Fig. 1 shows the result of a single run and the $3\sigma$ predicted standard deviations from a straight formulation of a Kalman filter. In order to show the equivalence between the Kalman filter (KF) and the UDU information approach (UDUI), Fig. 2 shows the norm of the difference between the two state estimates

$$\epsilon_{\mathbf{x}} = \|\hat{\mathbf{x}}_{KF} - \hat{\mathbf{x}}_{UDUI}\|$$

while Fig. 3 compares the Kalman filter covariance $P_{KF}$ with the UDU factorization of the Information matrix $P^{-1}_{UDUI} = UDU^T$ by plotting the following quantity:

$$\epsilon_P = \|P_{KF}\ P^{-1}_{UDUI} - I\|$$

The figures show that the proposed algorithm results closely match the Kalman filter hence validating the proposed algorithm as its UDU information formulation.

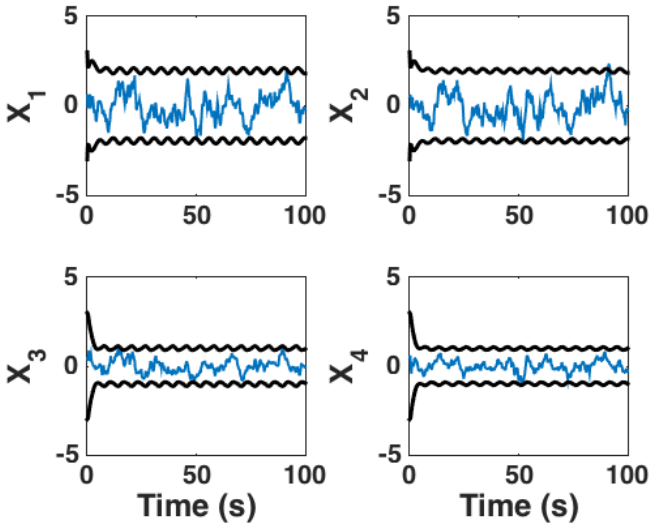


Fig. 1. Estimation Error and $3\sigma$ predicted standard deviations

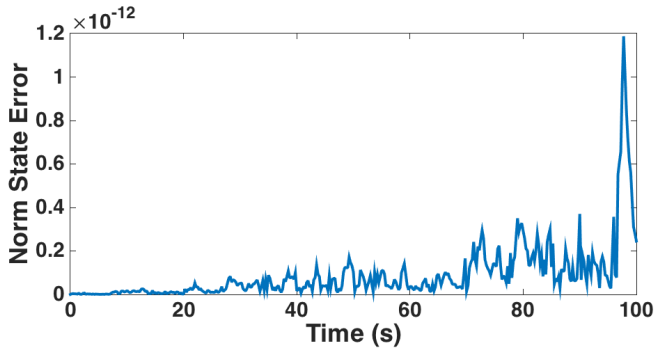


Fig. 2. Norm of the State Error ($\|\hat{\mathbf{x}}_{KF} - \hat{\mathbf{x}}_{UDUI}\|$)

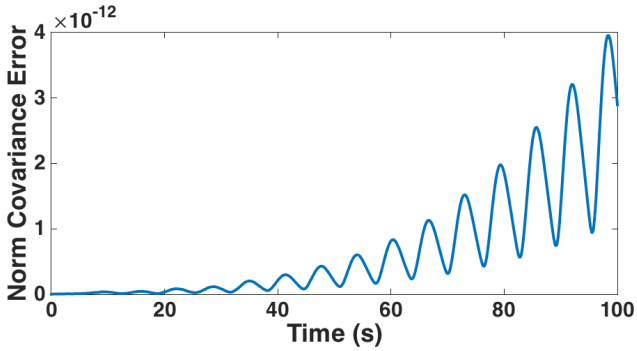


Fig. 3. Norm of the Covariance error ($\|P_{KF}\ P_{UDUI}^{-1} - I\|$)

## V. Conclusions

A new algorithmic mechanization of the classic Kalman filter is presented, the new algorithm combines the information formulation with the UDU factorization. While the covariance formulation of the Kalman filter is usually employed, the information formulation has distinct advantages in some applications, for example when no initial condition is available. The UDU factorization is a wildly adopted technique to produce a numerically stable and accurate algorithm to keep the covariance matrix symmetric and positive definite. A numerical example confirms the equivalency between the Kalman filter and the proposed algorithm.

## Acknowledgments

This work was supported in part by NASA JSC contract NNX17AI35A.

## References

[1] C. Thornton, "Triangular Covariance Factorizations for Kalman Filtering," Ph.D. dissertation, University of California at Los Angeles, October 1976.

[2] G. Bierman and C. Thornton, "Numerical comparison of kalman filter algorithms: Orbit determination case study," *Automatica*, vol. 13, pp. 23–25, 1977.

[3] G. J. Bierman, *Factorization Methods for Discrete Sequential Estimation*. New York: Dover Publications, 2006.

[4] S. Evans, W. Taber, T. Drain, J. Smith, H.-C. Wu, M. Guevara, R. Sunseri, and J. Evans, "Monte: The next generation of mission design and navigation software," *6th International Conference on Astrodynamics Tools and Techniques (ICATT)*, March 2016.

[5] J. Sud, R. Gay, G. Holt, and R. Zanetti, "Orion Exploration Flight Test 1 (EFT1) Absolute Navigation Design," in *Proceedings of the AAS Guidance and Control Conference*, ser. Advances in the Astronautical Sciences, vol. 151, Breckenridge, CO, January 31–February 5, 2014 2014, pp. 499–509, aAS 14-092.

[6] R. Kalman, "A new approach to linear filtering and prediction problems," *Trans. ASME (J. Basic Eng.)*, vol. 82D, pp. 34–45, March 1960.

[7] J. Potter and R. Stern, "Statistical filtering of space navigation measurements," *Proceedings of the AIAA Guidance and Control Conference*, 1963.

[8] R. Battin, *An Introduction to the Mathematics and Methods of Astrodynamics*. Reston, VA: AIAA, 1999.

[9] G. H. Golub and C. F. V. Loan, *Matrix Computations*, 2nd ed. Baltimore, MD: John Hopkins University Press, 1989, pp. 141–142.

[10] M. Verhaegen and P. Van Dooren, "Numerical aspects of different kalman filter implementations," *IEEE Transactions on Automatic Control*, vol. 31, no. 10, pp. 907–917, October 1986.

[11] P. Kaminski, A. Bryson, and S. Schmidt, "Discrete square root filtering: A survey of current techniques," *IEEE Transactions on Automatic Control*, vol. 16, no. 6, pp. 727–736, December 1971.

[12] Y. Oshman and I. Y. Bar-Itzhack, "Square root filtering via covariance and information eigenfactors," *Automatica*, vol. 22, no. 5, pp. 599–604, 1986.

[13] R. G. Brown and P. Y. Hwang, *Introduction To Random Signals And Applied Kalman Filtering*, 3rd ed. John Wiley and Sons, 1997, pp. 246–250.

[14] P. Maybeck, *Stochastic Models, Estimation and Control, Vol. 1*. New York, NY: Academic Press, 1979.

[15] ——, *Stochastic Models, Estimation and Control, Vol. 2*. New York, NY: Academic Press, 1979.

[16] P. Dyer and S. McReynolds, "Extension of square-root filtering to include process noise," *Journal of Optimization Theory and Applications*, vol. 3, no. 6, pp. 444–458, December 1969.

[17] G. Golub, "Numerical methods for solving linear least squares problems," *Numerische Mathematik*, vol. 7, no. 3, pp. 206–216, Jun 1965, doi: 10.1007/BF01436075.

[18] R. J. Hanson and C. L. Lawson, "Extensions and applications of the householder algorithm for solving linear least squares problems," *Mathematics of Computation*, vol. 23, no. 108, pp. 787–812, 1969.

[19] G. Bierman, "Sequential square root filtering and smoothing of discrete linear systems," *Automatica*, vol. 10, pp. 147–158, 1974.

[20] ——, "The treatment of bias in the square root information filter/smoother," *Journal of Optimization Theory and Applications*, vol. 16, no. 1/2, pp. 165–178, July 1975.

[21] C. Thornton and G. Bierman, "Gram-schmidt algorithms for covariance propagation," *IEEE Conference on Decision and Control*, pp. 489–498, 1975.

[22] W. Agee and R. Turner, "Triangular decomposition of a positive definite matrix plus a symmetric dyad with application to kalman filtering," *White Sands Missile Range Tech. Rep. No. 38*, 1972.

[23] N. Carlson, "Fast triangular factorization of the square root filter," *AIAA Journal*, vol. 11, no. 9, pp. 1259–1265, September 1973.